Journal Pre-proofs

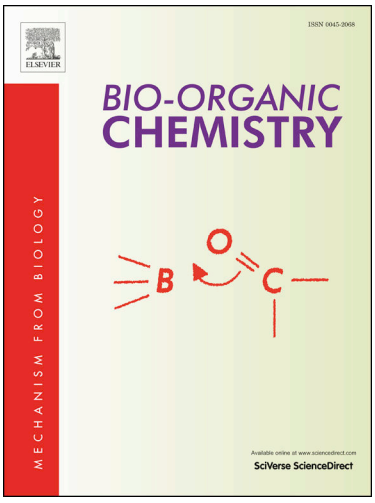

Structurally diverse diterpenoids from *Pieris japonica* as potent analgesics

Guijuan Zheng, Pengfei Jin, Lang Huang, Qihua, Zhang, Lingkui Meng, Guangmin Yao

PII: S0045-2068(20)30390-4
DOI: https://doi.org/10.1016/j.bioorg.2020.103794
Reference: YBIOO 103794

To appear in: *Bioorganic Chemistry*

Received Date: 18 February 2020
Revised Date: 18 March 2020
Accepted Date: 23 March 2020

Please cite this article as: G. Zheng, P. Jin, L. Huang, Qihua, Zhang, L. Meng, G. Yao, Structurally diverse diterpenoids from *Pieris japonica* as potent analgesics, *Bioorganic Chemistry* (2020), doi: https://doi.org/10.1016/j.bioorg.2020.103794

Structurally diverse diterpenoids from *Picris japonica* as potent analgesics

Guijuan Zheng, Pengfei Jin, Lang Huang, Qihua, Zhang, Lingkui Meng, Guangmin Yao*

Hubei Key Laboratory of Natural Medicinal Chemistry and Resource Evaluation, School of Pharmacy, Tongji Medical College, Huazhong University of Science and Technology, Wuhan 430030, People's Republic of China

* Corresponding author.

E-mail address: gyap@mail.hust.edu.cn (G. Yao).

A B S T R A C T

Sixteen diterpenoids (**1**−**16**) including 10 new ones, pierisjaponins A−J (**1**−**10**), were isolated and identified from *Pieris japonica*, and their structures were classified into eight diverse carbon skeletons. Pierisjaponins A (**1**) and B (**2**) represent the first 1,5-*seco*-grayanane diterpenoid glucosides and only showed 17 carbon resonances instead of 26 carbons in the ^{13}C NMR spectra, their structures were finally defined by single-crystal X-ray diffraction, and the unusual NMR phenomena were explained. Pierisjaponin E (**5**) is the first mollane diterpene glucoside. This is the first time to report *ent*-labdane (**3**, **4**, and **11**) and *ent*-rosane (**15**) type diterpenoids from the Ericaceae plants, which provided the precursors of the Ericaceae diterpenoids and enlarged the chemical diversity of Ericaceae diterpenoids. All the 16 isolates showed potent analgesic activities, and this is the first time to describe the analgesic activities of 1,5-*seco*-grayanane, *ent*-labdane, mollane, and *ent*-rosane type diterpenoids. A preliminary structure-activity relationship is discussed, which provided new clues to design novel analgesics based on the Ericaceae diterpenoids.

Keywords:

Pieris japonica (Thunb.) D. Don ex G. Don (Ericaceae)

Diterpenoids

Absolute configuration

Analgesics

Structure-activity relationship

1. Introduction

Diterpenoids from the Ericaceae family are characteristic for highly oxidized and polycyclic carbon skeletons, some of them showed anti-inflammatory [1], antiviral [2,3], neuroprotective and cAMP regulation [4], potassium channel moderator [5], antifeedant [6], PTP1B inhibitory [7-10], and analgesic activities [11-14]. To date, approximately 407 diterpenoids have been reported from the Ericaceae plants [15-17], and their carbon skeletons are classified into 25 types (Fig. 1), named grayanane [18], 1,5-*seco*-grayanane [19,20], 1,10-*seco*-grayanane [14,21], 3,4-*seco*-grayanane [22], 5,6-*seco*-grayanane [23], 9,10-*seco*-grayanane [24,25], 1,10:2,3-di*seco*-grayanane [3,14], 2,3:5,6-di*seco*-grayanane [8], leucothane [26], kalmane [27], 1,5-*seco*-kalmane [28], micranthane [29], mollane [30], rhodomollane [9], D-*homo*-grayanane [2], mollebenzylane [10], *ent*-kaurane [31,32], 4,5-*seco*-*ent*-kaurane [12,32,33], A-*homo*-B-*nor*-*ent*-kaurane [14,34], isopimarane [35], 6,7-*seco*-isopimarane [35], 14,15-di*nor*-9,10-*seco*-labdane [35], abietane [36], 17-*nor*-abietane [37], and 17,18-di*nor*-abietane [37]. Among them, grayanane type diterpenoids are the major and characteristic diterpenoids in Ericaceae plants, and their plausible biogenetic precursor is *ent*-kaurane type diterpene [15]. It has been proved that the *ent*-labdane type diterpene, directly derived from GGPP, is the precursor of the *ent*-pimarane type diterpene [38], and the *ent*-pimarane type diterpene generates the *ent*-kaurane type diterpene via the intermediate *ent*-beyerane type diterpene [39]. Thus, *ent*-labdane and labdane type diterpenoids should be the precursors of the Ericaceae diterpenoids.

However, there are no reports of any labdane, *ent*-labdane, *ent*-pimarane, *ent*-beyerane, or *ent*-rosane type diterpenoids from the Ericaceae plants, although 14,15-di*nor*-9,10-*seco*-labdane, isopimarane, and 6,7-*seco*-isopimarane type diterpenoids have been reported from *Lyonia ovalifolia* (Ericaceae) [35].

Among the reported diterpenoids from the Ericaceae family, grayanane [5,11-14,32,40-47], 1,10-*seco*-grayanane [14,21], 3,4-*seco*-grayanane [22,48,49], 1,10:2,3-di*seco*-grayanane [3,14],

A-*homo*-B-*nor*-*ent*-kaurane [14,34], kalmane [21,32,43], and micranthane [44] type diterpenoids were proved to exhibit obvious analgesic activities. Among them, grayanoids rhodojaponins III and VI from *Rhododendron molle* (Ericaceae) showed potent antinociceptive effects than morphine in the mice model of acute inflammatory pain [41]. However, there is no any reports of the analgesic activities of 1,5-*seco*-grayanane, mollane, *ent*-labdane, and *ent*-rosane type diterpenoids.

In a continuing search for structurally intriguing diterpenoids as analgesics from the Ericaceae plants [11-14,46,47], grayanane diterpenoids and grayanane diterpenoid glucosides with analgesic activities have been identified from *Pieris japonica* [46,47]. Further investigation led to the isolation of 16 diterpenoids (**1**−**16**) including 10 new ones, pierisjaponins A−J (**1**−**10**), from the leaves of *Pieris japonica*. The structures of 16 diterpenoids (**1**−**16**) were classified into eight diverse carbon skeletons, 1,5-*seco*-grayanane, *ent*-labdane, mollane, 4,5-*seco*-*ent*-kaurane, leucothane, 1,10:2,3-di*seco*-grayanane, *ent*-rosane, and kalmane, respectively (Fig. 2). Pierisjaponins A (**1**) and B (**2**) represent the first examples of 1,5-*seco*-grayanane diterpenoid glucosides. Pierisjaponins C (**3**) and D (**4**), and *ent*-manool (**11**) are first *ent*-labdane diterpenoids from Ericaceae plants. Pierisjaponin E (**5**) is the first mollane glucoside. Pierisformosides D (**13**) and G (**14**) and rhodomollein XIV (**16**) were characterized from *P. japonica* for the first time. 7-Deoxyrosenonolactone (**15**) is the first example of *ent*-rosane diterpenoid from Ericaceae family. It's the first report of *ent*-labdane and *ent*-rosane diterpenoids from the Ericaceae plants. All the isolates were tested for their analgesic activities, and **1**−**6**, **8**−**10**, and **12**−**15** showed distinct analgesic effects with inhibition rates of the writhing above 50% (5.0 mg/kg). Especially, even at the lower dose of 0.04 mg/kg, pierisjaponins B (**2**) and D (**4**), and 7-deoxyrosenonolactone (**15**) exhibited stronger analgesic activities than morphine (the positive drug) with inhibition rates of

1,5-*seco*-grayanane, mollane, *ent*-labdane, and *ent*-rosane diterpenoids.

2. Experimental section

2.1. General experimental procedures

HRMS (ESI-TOF) data were acquired on a Bruker micrOTOF II. Optical rotations were recorded in methanol using a Perkin-Elmer 341 polarimeter. Melting points were measured on a Beijing TechX-5 microscopic melting point apparatus. FT-IR spectra were measured using a Bruker Vertex 70 instrument. The UV data were obtained on a Varian Cary 50 spectrophotometer. ECD spectra were recorded on a JASCO J−810 spectrometer. NMR spectra were obtained on a Bruker AM-400 spectrometer, and the ^{1}H and ^{13}C NMR chemical shifts were referenced to the solvent residual peaks for methanol-d_4 at δ_H 3.31 and δ_C 49.15. The crystallographic data were obtained on a Bruker SMART APEX-II CCD diffractometer equipped with graphite-monochromatized Cu Kα radiation (λ = 1.54178 Å) for pierisjaponins A (**1**), C (**3**), and F (**6**) and Mo Kα radiation (λ = 0.71073 Å) for pierisjapanin G (**7**), respectively. Samples were purified by semipreparative HPLC using a Dionex P680 quaternary system with a UV detector and a HPLC column (5 μm, 10 × 250 mm, Welch Ultimate XB-C_{18} or XB-phenyl). GC was analyzed on an Agilent 7820A GC (30 m × 0.25 mm × 0.5 μm, Welch WM-1).

2.2. Plant material

The leaves of *Pieris japonica* (Thunb.) D. Don ex G. Don (Ericaceae) were collected in July 2014 at Baishanzu, Lishui, China, and authenticated by Prof. B.-Y. Ding at Wenzhou University.

2.3. Extraction and isolation

extract (6.7 kg) was yielded from the dried leaves of *P. japonica* (37.0 kg) after extraction at room temperature with 95%-ethanol and evaporation. The extract was then suspended in water and partitioned with CH_2Cl_2, EtOAc, and *n*-BuOH, respectively.

The CH_2Cl_2 fraction (1.1 kg, A) was chromatographed over a silica gel column eluting with CH_2Cl_2−Me_2CO (15:1 to 0:1) to give eleven fractions (A1−A11) based on the analysis of the TLC plates. These fractions were repeatedly separated and purified by a MPLC ODS column with MeOH−H_2O, Sephadex LH-20, and C_{18} HPLC to yield compounds **3** (8.7 mg), **7** (9.6 mg), **8** (39.6 mg), **9** (2.8 mg), and **10** (4.4 mg). The EtOAc fraction (426.5 g, B) was fractionated over a silica gel column with CH_2Cl_2−MeOH (50:1 to 2:1) to afford ten subfractions B1−B10 on the basis of the analysis of the TLC plates. Similar procedures were applied to these ten fractions B1−B10 to yield pure compounds **4** (19.0 mg), **12** (21.8 mg), and **14** (31.2 mg). The *n*-BuOH fraction (441.7 g, C) was applied to a silica gel column with CH_2Cl_2−MeOH (20:1 to 0:1) to afford six subfractions C1−C6 based on the analysis of the TLC spots. Similar procedures were applied to these six subfractions to afford diterpenoids **1** (21.0 mg), **2** (11.8 mg), **5** (28.8 mg), **6** (7.8 mg), **13** (26.4 mg), and **16** (18.8 mg).

2.4. Spectroscopic data

Pierisjaponin A (**1**): Colorless prisms (MeOH); mp 247−249 °C; $[\alpha]^{27}_D$ −59.1 (*c* 0.3, MeOH); UV (MeOH) λ_{max} (log ε): 235 (3.1) nm; IR ν_{max}: 3415, 2936, 1687, 1636, 1382, 1078, 1023, 927 cm^{-1} (KBr); CD (MeOH) λ_{max} ($\Delta\varepsilon$) = 232 (+2.3), 318 (−2.0) nm; for ^1H and ^{13}C NMR data, see Tables 1 and 2; HRESIMS *m/z* 537.2670 $[M + Na]^+$ (calcd for $C_{26}H_{42}O_{10}Na$, 537.2676) and 1051.5440 $[2M + Na]^+$ (calcd for $C_{52}H_{84}O_{20}Na$, 1051.5454).

Pierisjaponin B (**2**): Colorless oil; $[\alpha]^{27}_D$ −63.8 (*c* 0.2, MeOH); UV (MeOH) λ_{max} (log ε): 218 (3.0) nm; IR ν_{max}: 3410, 1639, 1388, 1080, 1040 cm^{-1} (KBr); CD (MeOH) λ_{max} ($\Delta\varepsilon$) = 230 (+2.4), 319 (−2.1) nm; for ^1H

and Na, 553.2625).

Pierisjaponin C (**3**): Colorless blocks (MeOH); mp 122−123 °C; $[\alpha]^{27}_D$ −38.6 (c 0.2, MeOH); UV (MeOH) λ_{max} (log ε): 207 (2.9) nm; IR ν_{max}: 3382, 2937, 2853, 1645, 1461, 1385, 1185, 1085, 1032, 918, 901 cm^{-1} (KBr); CD (MeOH) λ_{max} ($\Delta\varepsilon$) = 211 (+1.8) nm; for ^1H and ^{13}C NMR data, see Tables 1 and 2; HRESIMS *m/z* 345.2397 $[M + Na]^+$ (calcd for $C_{20}H_{34}O_3Na$, 345.2406).

Pierisjaponin D (**4**): Colorless oil; $[\alpha]^{27}_D$ −25.8 (*c* 0.1, MeOH); UV (MeOH) λ_{max} (log ε): 208 (2.9) nm; IR ν_{max}: 3409, 2936, 2867, 1643, 1389, 1169, 1079, 1049, 988, 928, 889 cm^{-1} (KBr); CD (MeOH) λ_{max} ($\Delta\varepsilon$) = 210 (+1.7) nm; for ^1H and ^{13}C NMR data, see Tables 1 and 2; HRESIMS *m/z* 507.2971 $[M + Na]^+$ (calcd for $C_{26}H_{44}O_8Na$, 507.2934).

Pierisjaponin E (**5**): White amorphous powder; $[\alpha]^{27}_D$ −12.9 (*c* 0.7, MeOH); UV (MeOH) λ_{max} (log ε): 202 (2.8) nm; IR ν_{max}: 3428, 2946, 1637, 1376, 1085, 1042, 981, 889 cm^{-1} (KBr); for ^1H and ^{13}C NMR data, see Tables 1 and 2; HRESIMS *m/z* 537.2676 $[M + Na]^+$ (calcd for $C_{26}H_{42}O_{10}Na$, 537.2676).

Pierisjaponin F (**6**): Colorless blocks (MeOH); mp 184−185 °C; $[\alpha]^{27}_D$ −52.5 (*c* 0.1, MeOH); UV (MeOH) λ_{max} (log ε): 200 (2.9) nm; IR ν_{max}: 3393, 2927, 2873, 1697, 1387, 1166, 1087, 1027 cm^{-1} (KBr); for ^1H and ^{13}C NMR data, see Tables 1 and 2; HRESIMS *m/z* 537.2695 $[M + Na]^+$ (calcd for $C_{26}H_{42}O_{10}Na$, 537.2676).

Pierisjaponin G (**7**): Colorless prisms (MeOH); mp 249−253 °C; $[\alpha]^{27}_D$ −4 (*c* 0.4, MeOH); UV (MeOH) λ_{max} (log ε): 207 (3.2) nm; IR ν_{max}: 3526, 3406, 2934, 1708, 1452, 1384, 1207, 1137, 1058, 967, 885 cm^{-1} (KBr); CD (MeOH) λ_{max} ($\Delta\varepsilon$) = 310 (−2.9) nm; for ^1H and ^{13}C NMR data, see Tables 3 and 2; HRESIMS *m/z* 357.1996 $[M + Na]^+$ (calcd for $C_{20}H_{30}O_4Na$, 357.2042).

Pierisjaponin H (**8**): Colorless oil; $[\alpha]^{27}_D$ −67.7 (*c* 0.3, MeOH); UV (MeOH) λ_{max} (log ε): 200 (3.1), 271 (2.8) nm; IR ν_{max}: 3398, 2937, 2871, 1696, 1452, 1376, 1225, 1120, 1028, 897 cm^{-1} (KBr); CD (MeOH) λ_{max} ($\Delta\varepsilon$) = 297 (−1.8) nm; for ^1H and ^{13}C NMR data, see Tables 3 and 2; HRESIMS *m/z* 343.2250 $[M + Na]^+$ (calcd for $C_{20}H_{32}O_3Na$, 343.2249) and 663.4646 $[2M + Na]^+$ (calcd for $C_{40}H_{64}O_6Na$, 663.4601).

(2.8) nm; IR ν_{max}: 3433, 2941, 1637, 1387, 1217, 1043 cm^{-1} (KBr); CD (MeOH) λ_{max} ($\Delta\varepsilon$) = 297 (−1.9) nm; for ^{1}H and ^{13}C NMR data, see Tables 3 and 2; HRESIMS *m/z* 359.2207 $[M + Na]^+$ (calcd for $C_{20}H_{32}O_4Na$, 359.2198) and 695.4528 $[2M + Na]^+$ (calcd for $C_{40}H_{64}O_8Na$, 695.4499).

Pierisjaponin J (**10**): Colorless oil; $[\alpha]^{27}_D$ +34.3 (*c* 0.4, MeOH); UV (MeOH) λ_{max} (log ε): 200 (2.7) nm; IR ν_{max}: 3387, 2936, 1761, 1704, 1440, 1388, 1136, 1037, 963 cm^{-1} (KBr); for ^{1}H and ^{13}C NMR data, see Tables 3 and 2; HRESIMS *m/z* 407.2052 $[M + Na]^+$ (calcd for $C_{20}H_{32}O_7Na$, 407.2046).

2.5. X-ray Crystallographic analysis.

The crystallographic data of pierisjaponins A (**1**) (CCDC 1970614), C (**3**) (CCDC 1970615), F (**6**) (CCDC 1970616), and G (**7**) (CCDC 1970617) have been stored in the Cambridge Crystallographic Data Centre. Their X-ray crystal structures are depicted in Figures 4−7.

Crystallographic data of pierisjaponin A (**1**): $C_{26}H_{42}O_{10}$, M = 514.59, 0.18 × 0.16 × 0.15 mm^3, V = 2549.9(7) $Å^3$, monoclinic, $P2_1$, Z = 4, wavelength: 1.54178 Å, radiation type: Cu Kα, T = 173(2) K, $\alpha = \gamma$ = 90°, β = 104.857(14)°, a = 6.8645(14) Å, b = 30.819(4) Å, c = 12.4698(15) Å, θ range for data collection 2.868 to 65.245°, absorption coefficient 0.848 mm^{-1}, F(000) = 1112, $-8 \le h \le 8$, $-36 \le k \le 36$, $-14 \le l \le 14$, completeness to θ (65.245°) 99.5%, 19393 reflections measured, 8565 independent reflections [$R_{(int)}$ = 0.0485], data/restraints/parameters 8565/1/707. The final R_1 = 0.0356 [$I > 2\sigma(I)$], the final wR_2 = 0.0764 [$I > 2\sigma(I)$]. The final (all data) R_1 = 0.0462, the final (all data) wR_2 = 0.0816. Hooft parameter 0.03(8), Flack parameter 0.01(8).

Crystallographic data of pierisjaponin C (**3**): $C_{20}H_{34}O_3$, M = 322.47, 0.22 × 0.20 × 0.18 mm^3, V = 1873.34(19) $Å^3$, monoclinic, C_12_1, Z = 4, wavelength: 1.54178 Å, radiation type: Cu Kα, T = 173(2) K, $\alpha = \gamma$ = 90°, β = 97.185(2)°, a = 24.626(15) Å, b = 7.4516(4) Å, c = 10.2893(6) Å, θ for data collection 4.331 to 68.267°, absorption coefficient 0.583 mm^{-1}, F(000) = 712, $-29 \le h \le 28$, $-8 \le k \le 8$, $-12 \le l \le 12$,

0.0559], data/restraints/parameters 3404/21/218. The final R_1 = 0.0513 [$I > 2\sigma(I)$], the final wR_2 = 0.1453 [$I > 2\sigma(I)$]. The final (all data) R_1 = 0.0519, the final (all data) wR_2 = 0.1461. Hooft parameter 0.06(5), Flack parameter −0.04(4).

Crystallographic data of pierisjaponin F (**6**): $C_{26}H_{42}O_{10}\cdot 4(H_2O)$, M = 586.65, 0.30 × 0.20 × 0.10 mm^3, V = 3000.7(3) Å^3, orthorhombic, $P2_12_12_1$, Z = 4, wavelength: 1.54178 Å, radiation type: Cu Ka, T = 173(2) K, α = 90°, β = 90°, γ = 90°, a = 6.2405(3) Å, b = 8.3505(4) Å, c = 57.583(3) Å, θ for data collection 5.35 to 66.87°, absorption coefficient 0.883 mm^{-1}, F(000) = 1268, $-7 \le h \le 7$, $-9 \le k \le 9$, $-47 \le l \le 68$, completeness to θ (66.91°) 99.3%, 5276 reflections measured, 4600 independent reflections [$R_{(int)}$ = 0.0406], data/restraints/parameters 5276/374/330. The final R_1 = 0.0448 [$I > 2\sigma(I)$], the final wR_2 = 0.1121 [$I > 2\sigma(I)$]. The final (all data) R_1 = 0.0539, the final (all data) wR_2 = 0.1172. Hooft parameter 0.0(1), Flack parameter −0.1(2).

Crystallographic data of pierisjaponin G (**7**): $C_{20}H_{30}O_4$, M = 334.44, 0.20 × 0.18 × 0.12 mm^3, V = 848.6(8) Å^3, monoclinic, $P2_1$, Z = 2, wavelength: 0.71073 Å, radiation type: Mo Ka, T = 298(2) K, $\alpha = \gamma$ = 90°, β = 91.483(16)°, a = 6.106(4) Å, b = 11.149(6) Å, c = 12.468(7) Å, θ for data collection 3.27 to 25.01°, absorption coefficient 0.089 mm^{-1}, F(000) = 264, $-7 \le h \le 7$, $-13 \le k \le 13$, $-14 \le l \le 14$, completeness to θ (25.01°) 97.9%, 2847 reflections measured, 2720 independent reflections [$R_{(int)}$ = 0.0545], data/restraints/parameters 2847/1/222. The final R_1 = 0.1191 [$I > 2\sigma(I)$], the final wR_2 = 0.2637 [$I > 2\sigma(I)$]. The final (all data) R_1 = 0.1161, the final (all data) wR_2 = 0.2611.

2.6. Acid hydrolysis and GC analysis.

Pierisjaponin A (**1**) was hydrolyzed by HCl (2 mM), the trimethylsilylthiazolidine derivative of the hydrate was prepared, and the GC analysis was performed according to the procedures described previously [50,51]. The GC retention times of the derivatives of the standards D- and L-glucoses and the hydrate of **1**

times of the derivatives of the hydrates of **2** and **4**−**6** were 14.802, 14.798, 14.818, and 14.789 min (Figs. S15−S18), respectively. Therefore, the D-glucose unit in pierisjaponins A (**1**), B (**2**), and D−H (**4**−**6**) was determined.

2.7. ECD calculation

The ECD calculation methods of pierisjaponins G (**7**) and (**8**) were performed as described previously [14]. The detailed methods were also depicted in the Supplementary Information.

2.8. Analgesic activities assay.

All the diterpenoids **1**−**16** were tested for analgesic activities in mice according to the procedures previously described [41,46].

3. Results and discussion

*3.1. Structural elucidations of pierisjaponins A−J (**1**−**10**)*

Pierisjaponin A (**1**), colorless prisms with a mp of 247−249 °C, was assigned a molecular formula of $C_{26}H_{42}O_{10}$ with six degrees of unsaturation on the basis of the HRESIMS $[M + Na]^+$ and $[2M + Na]^+$ ions at *m/z* 537.2670 (calcd for $C_{26}H_{42}O_{10}Na$, 537.2676) and 1051.5440 (calcd for $C_{52}H_{84}O_{20}Na$, 1051.5454), respectively. The characteristic UV absorption at 235 nm (log ε = 3.1) and the IR absorption at 1687 cm^{-1} indicated the existence of a carbonyl (C=O). The ^1H NMR spectroscopic data (Table 1) in CD_3OD at room temperature of **1** showed the resonances for four methyls (δ_H 1.36, 1.34, 1.40, and 2.05), two oxygenated methines (δ_H 3.83 and 4.23), and a typical glucopyranosyl group [δ_H 4.48 (d, H-1′), 3.85 (dd, H-6′a), and 3.68 (dd, H-6′b)] [51]. However, it was very strange that the ^{13}C NMR spectrum obtained in CD_3OD at room temperature only showed 17 carbon resonances assignable to a carbonyl carbon (δ_C 214.5), a sp^3 quaternary carbon (δ_C 50.2), an oxygenated tertiary carbon (δ_C 80.4), seven methines including five oxygenated (δ_C 49.5,

56.8, 70.7, 71.4, 75.8, 77.6, and 78.3), five methylenes (δ_C 23.9, 27.0, 36.5, 58.4, and 62.4), and two methyls

(δ_C 24.3 and 17.3) by the DEPT spectrum, instead of 26 carbons as indicated by the HRESIMS data.

2D NMR analysis were attempted to certificate the remaining carbon resonances and delineate the structure of pierisjaponin A (**1**) (Fig. 3). An oxymethine carbon C-3 (δ_C 93.9), a methylene C-7 (δ_C 48.4), and an anomeric carbon C-1′ (δ_C 106.0) were disclosed by the HSQC spectrum. The ^{1}H–^{1}H COSY data signified three substructures: (a) CH-6/CH_2-7, (b) CH-9/CH_2-11/CH_2-12/CH-13/CH_2-14, and (c) CH-1′/CH-2′/CH-3′/CH-4′/CH-5′/CH_2-6′. The observed HMBC correlations from H_3-17 to C-13/C-15/C-16, H_2-15 to C-8/C-9/C-14, H_2-14 to C-8/C-9, and H_2-7 to C-9 constructed the rings B and C. Correlations from H_3-20 to C-9 (δ_C 56.8), C-1 (δ_C 128.1), and C-10 (δ_C 146.0) in the HMBC experiment demonstrated the existence of an endocyclic double bond $\Delta^{1(10)}$. The linkages of C-3/C-5/C-18/C-19 to C-4 and the carbon signals of C-4, C-18, and C-19 were assigned by HMBC correlations from the *gem*-methyls [(δ_H 1.34, s, H_3-18) and (δ_H 1.40, s, H_3-19)] to C-3/C-4/C-5. The glycosylation position was determined at C-3 by the key HMBC correlations from the anomeric proton δ_H 4.48 (H-1′) to C-3. A carbonyl group, a double bond $\Delta^{1(10)}$, and a glycose unit accounted for three degrees of unsaturation, suggesting that pierisjaponin A (**1**) was a tricyclic diterpenoid glucoside. However, the ring A could not be constructed due to the lack of key correlation of H-2/C-2 and the connection of C-5/C-6.

The relative configuration of pierisjaponin A (**1**) was ascertained by the analysis of NOESY experiment. The NOESY cross-peaks of H-3/H-6, H-6/H_3-19, H_3-19/H-3, and H_3-19/H-2 (δ_H 4.67, br s) revealed that they were cofacial and assigned randomly as α-orientations (Fig. 3). The *cis*-fused rings B and C and H_3-17β orientation were determined by the cross signals of H-9/H-15β, H-11β/H_3-17, and H-15β/H_3-17.

To determine the absolute configuration of the sugar unit in pierisjaponin A (**1**), we hydrolyzed **1** using HCl and then prepared the trimethylsilylthiazolidine derivative of the hydrolysate of **1** [11,51]. The D-absolute configuration of the sugar unit in **1** was defined by comparison of the GC retention time of the derivative of the hydrolysate of **1** (t_R 14.764 min) with those of the standards (D-Glc, t_R 14.840 min; L-Glc, t_R 15.062 min). The large coupling constant 7.6 Hz of H-1′ indicated the β-linkage of the glycose in **1** [47].

Eventually, the complete structure of pierisjaponin A (**1**) was unambiguously constructed by X-ray diffraction analysis, and the Flack parameter [52] 0.01(8) and Hooft parameter [53] 0.03(8) defined its absolute configuration as shown in Fig. 4.

A molecular formula of $C_{26}H_{42}O_{11}$ (calcd for $C_{26}H_{42}O_{11}Na$, 553.2625) was ascertained to pierisjaponin B (**2**) by the positive $[M + Na]^+$ ion at *m/z* 553.2638 in the HRESIMS spectrum, suggesting one more oxygen atom than pierisjaponin A (**1**). The NMR data (Tables 1 and 2) of pierisjaponin B (**2**) shared great similarities of **1**, except for the presence of an oxymethine (δ_H 4.26, s, H-14; δ_C 80.8, C-14) in **2**, which replaced a methylene (δ_H 2.03, 1.73, H_2-14β; δ_C 36.5, C-14) in **1**. Thus, pierisjaponin B (**2**) was a 14-oxygenated product of **1**. The HMBC correlations (Fig. S1, Supplementary Information, SI) from H-14 (δ_H 4.26) to C-16 (δ_C 81.6), C-15 (δ_C 57.3), and C-12 (δ_C 27.6) further proved this deduction. Similar to **1**, H-3 in pierisjaponin B (**2**) was α-oriented. Cross-peaks of H-3/H-6 and H-6/H-14 in the NOESY experiment delineated the α-orientations of H-6 and H-14. Therefore, the structure of pierisjaponin B (**2**) was defined as 3β-(β-D-glucopyranosyloxy)-2β,6β,14β,16α-tetrahydroxy-1,5-*seco*-grayan-1(10)-en-5-one. The tendency of the ECD curve of pierisjaponin B (**2**) was similar to that of pierisjaponin A (**1**) (Fig. S2, SI), indicating their same absolute configuration, ignoring C-14.

1,5-*Seco*-grayanane diterpenoids are relatively rare in nature, heretofore, total five 1,5-*seco*-grayanane diterpenoid aglycones, grayanols A and B [54], grayanotoxins XXI [20] and XXII [55], and 3*S*,6*R*,14*R*,16*R*-tetrahydroxy-5-oxo-5,10-*seco*-*ent*-kaur-1(10)-ene [56], were reported from nature. Pierisjaponins A (**1**) and B (**2**) represent the first 1,5-*seco*-grayanane diterpenoid glucosides. A major feature of the 1,5-*seco*-grayanane diterpenoids is a ten-membered carbon ring system involving C-1−C-10, which is flexible and would lead to the co-existence of a number of transformable conformers in the solvents at room temperature [57]. The anisotropisations of the endocyclic double bond $\Delta^{1(10)}$ and the carbonyl C-5 in pierisjaponins A (**1**) and B (**2**) would result in different chemical shifts of C-1, C-2, C-3, C-5, C-7, C-10, C-20, and C-1′ in different conformers, and their chemical shifts differences were so big that the resonances were not obvious in the ^{13}C NMR experiment in CD_3OD at room temperature [23]. Likewise, H-1, H-2, H-3, H-6, and H-7 in the ^1H

NMR spectra of pierisjaponins A (**1**) and B (**2**) in CD_3OD showed weak and broad peaks, instead of resolved sharp peaks. While, the rigid and caged B and C rings fixed C-8 and C-9 so that the resonances of C-8, C-9, and C-11−C-17 could be ascertained obviously in the ^{13}C NMR experiments of pierisjaponins A (**1**) and B (**2**) at room temperature in CD_3OD. The NMR experiments at a lower temperature may improve the resolution of the NMR spectra [57]. There is no report of the unsual NMR phenomena of the 1,5-*seco*-grayanane diterpenoid aglycones, the unsual NMR phenomena of pierisjaponins A (**1**) and B (**2**) should arise from the presence of 2β-OH and the β-D-glucopyranosyl unit, which increased the complexity of the transformable conformers of the ten-membered carbon ring.

Pierisjaponin C (**3**), colorless blocks with a mp of 122−123 °C, has a molecular formula of $C_{20}H_{34}O_3$ as deduced from the NMR data and the HRESIMS $[M + Na]^+$ ion at *m/z* 345.2397 (calcd for $C_{20}H_{34}O_3Na$, 345.2406), having two more oxygen atoms than that of *ent*-manool (**11**). The NMR data (Tables 1 and 2) of pierisjaponin C (**3**) showed similarities to those of *ent*-manool (**11**) [58], a known labdane diterpenoid, and the main differences were the existence of an oxymethine (δ_H 3.18, dd, H-3; δ_C 79.7, C-3) and an oxymethylene (δ_H 3.38, 3.42, H_2-16; δ_C 69.8, C-16) in **3**, rather than the methylene (δ_H 1.39, 1.21, overlap, H_2-3; δ_C 43.5, C-3) and the methyl (δ_H 1.23, s, H-16; δ_C 27.6, C-16) in **11**. Thus, pierisjaponin C (**3**) should be a 3,16-dioxygenated derivative of *ent*-manool (**11**). The HMBC correlations (Fig. S3, SI) from the *gem*-methyls [δ_H 0.76 (s, H_3-19) and 0.97 (s, H_3-18)] to C-3 and from H_2-16 to C-14 (δ_C 143.1), C-13 (δ_C 77.3), and C-12 (δ_C 37.2) supported the planar structure of pierisjaponin C (**3**). The relative configuration of pierisjaponin C (**3**) was established by the NOESY experiment and the coupling constants analysis. The large coupling constants $J_{H\text{-}3/H\text{-}2}$ = 9.1 and 7.0 Hz characterized the axial orientation of H-3, namely β-orientation. The NOESY cross-peaks of H-3/H-5, H-5/H-9, and H-3/H_3-18 established the β-orientations of H-5, H-9, and H_3-18. The α-orientation of H_3-20 was determined by the NOESY correlation of H_3-20 and H_3-19α. However, it is hard to define the configuration of C-13 in the side chain. The gross structure of pierisjaponin C (**3**) was finally defined to be 3α,13α,16-trihydroxy-*ent*-labda-8(17),14(15)-diene via

pierisjaponin C (**3**) by a Flack parameter of −0.04(4) [52].

The HRESIMS $[M + Na]^+$ ion at *m/z* 507.2971 (calcd for $C_{26}H_{44}O_8Na$, 507.2934) and the NMR data assigned a molecular formula of $C_{26}H_{44}O_8$ to pierisjaponin D (**4**). The NMR data (Tables 1 and 2) of pierisjaponin D (**4**) and pierisjaponin C (**3**) shared closely similarities. However, the main difference was an additional glucose unit [δ_H 4.26 (d, H-1′), 3.87 (dd, H-6′a), and 3.66 (dd, H-6′b); δ_C 105.1, 78.1, 78.0, 75.3, 71.8, and 62.9] [47] in **4**. Thus, pierisjaponin D (**4**) should be a glucoside of pierisjaponin C (**3**). The C-16 glycosylation position was fixed by the de-shielded C-16 (δ_C 77.4) in **4** by 7.6 ppm compared to that (δ_C 69.8) in **3**, which was further ascertained by the HMBC correlations (Fig. S4, SI) from H-1′ (δ_H 4.26) to C-16 and from H_2-16 to C-1′ (δ_C 105.1). The ECD spectrum of pierisjaponin D (**4**) was almost identical to that of pierisjaponin C (**3**) (Fig. S5, SI), suggesting their same absolute configuration, ignoring the glucose unit in **4**. Similar to pierisjaponin A (**1**), the *β*-D-glucose unit in pierisjaponin D (**4**) was determined by chemical methods and GC analysis, as well as the large coupling constant J = 7.7 Hz of H-1′. Therefore, the structure of pierisjaponin D (**4**) was defined as 16-(*β*-D-glucopyranosyloxy)-3*α*,13*α*-dihydroxy -*ent*-labda-8(17),14(15)-diene.

Pierisjaponins C (**3**) and D (**4**) and *ent*-manool (**11**) are the first *ent*-labdane diterpenoids from the Ericaceae family. The bicyclic *ent*-labdane diterpenoids are considered to be the precursors of the Ericaceae diterpenoids (Fig. 1).

Pierisjaponin E (**5**) gave a molecular formula of $C_{26}H_{42}O_{10}$ as disclosed by the positive HRESIMS $[M + Na]^+$ ion at *m/z* 537.2676 (calcd for $C_{26}H_{42}O_{10}Na$, 537.2676), along with the ^{13}C NMR data. The 1D NMR data (Tables 1 and 2) of pierisjaponin E (**5**) showed some similarities to mollanol A [30], the first mollane (C-*nor*-D-*homo*-grayanane) type diterpenoid from *Rhododendron molle* (Ericaceae) and its structure was determined by single crystal X-ray diffraction, except for a

an oxygenated tertiary carbon C-10 (δ_C 72.4) and a sp^3 methine (δ_H 1.92, H-1; δ_C 52.4, C-1) in **5** replaced the tetra-substituted double bond $\Delta^{1(10)}$ [δ_C 138.1 (C-1) and 127.7 (C-10)] in mollanol A, and a methylene (δ_C 33.0, C-14) in **5** replaced the oxygenated methine (δ_C 78.4, C-14) in mollanol A. Thus, pierisjaponin E (**5**) was a 1(10)-hydrate-14-deoxy glucoside of mollanol A. Two substructures CH_2-11–CH_2-12–CH-13–CH_2-14 and CH-1/CH_2-2/CH-3 (Fig. S6, SI) were ascertained by the ^1H–^1H COSY data of pierisjaponin E (**5**). HMBC correlations from H_3-20 to C-10 (δ_C 72.4), C-9 (δ_C 53.9), and C-1 (δ_C 52.4) supported the linkages of C-1/C-9/C-20 through C-10. Similarly, the glycosylation position at C-3 was established by the HMBC correlations from the H-1′ (δ_H 4.24) to C-3 (δ_C 89.1) and from H-3 (δ_H 3.59) to the anomeric carbon C-1′ (δ_C 105.9). Similar to mollanol A, the downfield shifted C-8 (δ_C 84.4) and C-5 (δ_C 93.7), as well as the hydrogen deficiency of **5**, revealed an oxygen bridge between C-5 and C-8. H-1 was randomly assigned as α-orientation in pierisjaponin E (**5**). The correlations of H-1α/H-6, H_3-19/H-6, and H_3-20/H-6 in the NOESY experiment (Fig. S6, SI) verified that H-6, H_3-19, and H_3-20 were cofacial. The strong NOESY correlation of H-3/H_3-19α and weak NOESY correlation of H-3/H_3-18β indicated the α-orientation of H-3. The *cis*-fused C and D rings and H_3-17β orientation were identical to mollanol A. Similar to mollanol A [30], the β-orientation of the C-5-O-C-8 oxygen bridge was assigned. Similar to pierisjaponin A (**1**), the β-D-glucose unit in pierisjaponin E (**5**) was established. Consequently, pierisjaponin E (**5**) was defined as 3β-(β-D-glucopyranosyloxy)-6β,10β,16α-trihydroxy- 5β,8β-epoxy-C-*nor*-D-*homo*-grayanane. To date, only one mollane diterpenoid aglycone was reported, and pierisjaponin E (**5**) is the first mollane diterpenoid glucoside.

Pierisjaponin F (**6**) was yielded as a colorless block, mp 184−185 °C. Based on the HRESIMS [M + Na]$^+$ ion peak at *m/z* 537.2695 (calcd for $C_{26}H_{42}O_{10}Na$, 537.2676) and the ^{13}C NMR data, the molecular formula of pierisjaponin F (**6**) was assigned as $C_{26}H_{42}O_{10}$. The 1D NMR data (Tables 1

diterpenoid reported from *Rhododendron auriculatum* (Ericaceae). However, the main differences were the presence of an oxymethylene (δ_H 4.23, 3.53, each d, H_2-17; δ_C 75.1, C-17) and a glucopyranosyl group (δ_H 4.29, d, J = 7.7 Hz, H-1′; δ_C 105.5, 78.2, 78.0, 75.4, 71.8, 62.9) [51] in **6**, replacing the methyl (δ_H 1.36, s, H_3-17; δ_C 24.5, C-17) in rhodoauriculatol H. Consequently, pierisjaponin F (**6**) is a 17-oxygenated glucoside of rhodoauriculatol H. Combination of the chemical shift of C-17 (δ_C 75.1) and HMBC correlations (Fig. S7, SI) from H_2-17 to C-13/C-15/C-16/C-1′ (δ_C 105.5) and from H-1′ (δ_H 4.29) to C-17 proved the above deduction. Similar to pierisjaponin A (**1**), 2D NMR experiments, chemical methods, as well as GC analysis defined the structure of pierisjaponin F (**6**) as 17-(*β*-D-glucopyranosyloxy)-3*β*,10*β*,16*α*-trihydroxyleucothan-5-one, which was eventually supported by X-ray diffraction analysis (Fig. 6). The calculated Hooft parameter 0.0(1) [53] and Flack parameter −0.1(2) [52] was used to assign the absolute configuration (1*S*,3*S*,6*R*,8*R*,9*R*,10*R*,13*R*,16*R*,1′*R*,2′*R*,3′*S*,4′*S*,5′*R*) to pierisjaponin F (**6**).

A molecular formula of $C_{20}H_{30}O_4$ was assigned to pierisjaponin G (**7**) based on the ^{13}C NMR data and the HRESIMS $[M + Na]^+$ data at *m/z* 357.1996 (calcd for $C_{20}H_{30}O_4Na$, 357.2042). Comparison of the 1D NMR data of pierisjaponin G (**7**) and pierisformoside D (**13**) [59] (Tables 2 and 3) indicated that **7** and **13** shared a similar structure. The main differences were the missing glucose group and the shielding of C-3 (δ_C 77.6) in **7** compared to **13** (δ_C 86.3). Thus, pierisjaponin G (**7**) is an aglycone of pierisformoside D (**13**). Similar to **13**, H-1 in pierisjaponin G (**7**) was assigned as a *β*-orientation. Cross-peaks of H-1*β*/H-9, H-9/H-15b, and H-15b/H_3-17 in the NOESY experiment (Fig. S8, SI) determined the *β*-orientations of H-9 and H_3-17. The relative configuration of pierisjaponin G (**7**) was finally determined as (1R^*,3S^*,6S^*,8S^*,9R^*,13R^*,16R^*) by X-ray crystallographic analysis with Mo K*α* radiation (Fig. 7). The experimental ECD curve (Fig. 8) of pierisjaponin G (**7**) was similar to the calculated ECD curve of (1*R*,3*S*,6*S*,8*S*,9*R*,13*R*,16*R*)-**7** and

determined as 1*R*,3*S*,6*S*,8*S*,9*R*,13*R*,16*R*.

The HRESIMS $[M + Na]^+$ and $[2M + Na]^+$ ions at *m/z* 343.2250 (calcd for $C_{20}H_{32}O_3Na$, 343.2249) and 663.4646 (calcd for $C_{40}H_{64}O_6Na$, 663.4601), respectively, disclosed a molecular formula of $C_{20}H_{32}O_3$ to pierisjaponin H (**8**). The 1D NMR data of pierisjaponin H (**8**) (Tables 2 and 3) shared high similarities to those of pierisformoside G (**14**), a 4,5-*seco*-*ent*-kaurane diterpenoid glucoside [33], excepted for the absence of the glucose moiety and the shielding of C-19 (δ_C 65.9) in **8**, implying that pierisjaponin H (**8**) is an aglycone of pierisformoside G (**14**). Detailed 2D NMR data furnished the structure of pierisjaponin H (**8**) as 16*α*,19-dihydroxy-4,5-*seco*-*ent*-kaur-4(18)-en-5-one (Fig. S9, SI). Comparison of the experimental ECD curve of pierisjaponin H (**8**) and the calculated ECD curves of (8*S*,9*R*,10*S*,13*R*,16*R*)-**8** and its enantiomer ultimately defined its absolute configuration as 8*S*,9*R*,10*S*,13*R*,16*R* (Fig. 9).

Pierisjaponin I (**9**) possessed a molecular formula of $C_{20}H_{32}O_4$ based on the HRESIMS $[M + Na]^+$ and $[2M + Na]^+$ ions at *m/z* 359.2207 (calcd for $C_{20}H_{32}O_4Na$, 359.2198) and 695.4528 (calcd for $C_{40}H_{64}O_8Na$, 695.4499), respectively, suggesting one more oxygen atom than pierisjaponin H (**8**). The NMR data (Tables 2 and 3) of pierisjaponin I (**9**) were extremely similar to those of pierisjaponin H (**8**), while the main difference was that the oxymethine (δ_H 4.50, dd, J = 13.4, 6.0 Hz, H-6; δ_C 71.9, C-6) in **9** replaced a sp^3 methylene (δ_H 2.70, 2.24, H_2-6; δ_C 38.2, C-6) in **8**. Thus, pierisjaponin I (**9**) is a 6-oxygenated derivative of **8**, which was confirmed by the partial structure "–CHOH-6–CH_2-7–" (Fig. S10, SI) deduced from the $^1H-^1H$ COSY data and the de-shielding of C-6 (δ_C 71.9) in **9** compared to **8** (δ_C 38.2). Similar to **8**, H_3-20 in pierisjaponin I (**9**) was assigned as *α*-orientation. Correlation of H-6/H_3-20*α* in the NOESY experiment revealed the *α*-orientation of H-6. Thus, the structure of pierisjaponin I (**9**) was identified as 6*β*,16*α*,19-trihydroxy-4,5-*seco*-*ent*-kaur-4(18)-en-5-one. The ECD spectrum of pierisjaponin I (**9**)

configuration.

The molecular formula of pierisjaponin J (**10**) was assigned as $C_{20}H_{32}O_7$ based on the HRESIMS $[M + Na]^+$ ion at *m/z* 407.2052 (calcd for $C_{20}H_{32}O_7Na$, 407.2046). The NMR data of pierisjaponin J (**10**) (Tables 2 and 3) showed close similarities to those of mollolide A [3], a known di*seco*-grayanane diterpenoid from *Rhododendron molle* (Ericaceae), with the major difference of a methylene (δ_H 1.57, 1.71, H_2-12; δ_C 25.9, C-12) in **10**, replacing the oxymethine (δ_H 4.31, H-12; δ_C 68.7, C-12) in mollolide A. Thus, pierisjaponin J (**10**) should be a 12-deoxy product of mollolide A. The chemical shift δ_C 25.9 (C-12) and the HMBC correlations (Fig. S11, SI) from H-14/H-9 to C-12 (δ_C 25.9) fixed the above deduction. Consequently, the gross structure of **10** was deduced as 2,5*β*,14*β*,16*α*-tetrahydroxy-1,10:2,3-di*seco*-grayan-3,6*β*-olide-10-one. Detailed 2D NMR analysis and the biogenetic relationship supported this conclusion. To date, only two 1,10:2,3-di*seco*-grayanane diterpenoids, mollolide A [3] and rhodoauriculatol D [14], have been reported, and pierisjaponin J (**10**) represents the third 1,10:2,3-di*seco*-grayanane diterpenoid.

Six known diterpenoids **11**−**16** were identified as *ent*-manool (**11**) [58], pieroside B (**12**) [60], pierisformosides D (**13**) [59] and G (**14**) [33], 7-deoxyrosenonolactone (**15**) [61], and rhodomollein XIV (**16**) [62], respectively, by NMR data analysis and comparison to the reported data. Importantly, five known diterpenoids **11** and **13**−**16** were firstly reported from *P. japonica*. Except for pieroside B (**12**), all the other diterpenoids from *P. japonica* enlarged the chemical diversity of diterpenoids from the Ericaceae plants.

3.2. Analgesic activity

Since the grayanane and relevant diterpenoids from Ericaceae family have been proved to exhibited distinct analgesic activities [11,13,41], the diterpenoids **1**−**16** were tested for their analgesic activities in mice. Compared to the vehicle (***$p < 0.001$), diterpenoids **1**−**16** expressed analgesic

activities (Fig. 10). 1,5-*Seco*-grayanane (**1** and **2**), *ent*-labdane (**3** and **4**), mollane (**5**), leucothane (**6**, **12**, and **13**), 4,5-*seco*-*ent*-kaurane (**8**, **9**, and **14**), 1,10:2,3-di*seco*-grayanane (**10**), and *ent*-rosane (**15**) diterpenoids exhibited significant analgesic activities with the writhe inhibitions above 50% (5.0 mg/kg, i.p.). Even at a lower dose of 0.04 mg/kg, pierisjaponins B (**2**) and D (**4**) and 7-deoxyrosenonolactone (**15**) exhibited stronger analgesic effects than morphine with inhibition percentages of 66.2%, 64.8%, and 59.2%, respectively. It is the first time to report the analgesic activities of 1,5-*seco*-grayanane, mollane, *ent*-labdane, and *ent*-rosane diterpenoids.

3.3. Structure-activity relationships analysis

1,5-*Seco*-grayanane glucosides pierisjaponins A (**1**) and B (**2**) showed almost equivalent analgesic effects at a dose of 5.0 mg/kg with the inhibition rates of the writhes of 85.9%, and also showed significant analgesic activities even at a lower dose of 1.0 mg/kg with the writhe inhibition rates of 59.2% and 77.5%, respectively. Pierisjaponin B (**2**) with 14*β*-OH exhibited stronger analgesic effects than pierisjaponin A (**1**) without 14*β*-OH, implying that 14*β*-OH group may be conducive to the analgesic activity in the 1,5-*seco*-grayanane glucosides. Pierisjaponin C (**3**) bearing 3*α*-OH and 16-OH groups exhibited stronger analgesic effects than *ent*-manool (**11**) without 3*α*-OH and 16-OH groups, suggesting the stimulating effects of the 3,16-dihydroxy groups in the *ent*-labdane diterpenoids. Pierisjaponin D (**4**) possessing a glucose unit at C-16 showed more potent analgesic activities than the aglycone pierisjaponin C (**3**) with the writhe inhibition percentages of 83.1%, 73.2%, and 64.8% at doses of 1.0, 0.2, and 0.04 mg/kg, respectively, indicating 16-*O*-*β*-D-glucoside is a stimulating group. Leucothane type diterpenoid pierisjaponin F (**6**) with 10*β*-OH group exhibited stronger analgesic effects than leucothane type diterpenoids **7**, **12**, and **13** without 10*β*-OH, indicating that the 10*β*-OH group may enhance the analgesic effect in the leucothane type diterpenoids, which was agreement with the previous conclusions to the analgesic activities of leucothane diterpenoids [14]. The 4,5-*seco*-*ent*-kaurane diterpenoid aglycone pierisjaponin H (**8**)

indicating that 19-*O*-*β*-D-glucoside may be the deactivating moiety in the 4,5-*seco*-*ent*-kaurane diterpenoids.

4. Conclusions

In summary, 16 diterpenoids including ten new ones with eight different carbon skeletons were identified from the leaves of *P. japonica*. Pierisjaponins A (**1**) and B (**2**) represent the first 1,5-*seco*-grayanane diterpenoid glucosides. Pierisjaponins C (**3**) and D (**4**), and *ent*-manool (**11**) are the first *ent*-labdane diterpenoids from Ericaceae family. Pierisjaponin E (**5**) is the first mollane glucoside. Pierisformosides D (**13**) and G (**14**) and rhodomollein XIV (**16**) were firstly described from *P. japonica*. 7-Deoxyrosenonolactone (**15**) is the first *ent*-rosane diterpenoid from the Ericaceae family. Importantly, this is the first report of *ent*-labdane and *ent*-rosane diterpenoids from the Ericaceae plants, which enlarges the chemical diversity of Ericaceae diterpenoids. All the diterpenoids **1**−**16** expressed analgesic activities. Among them, 1,5-*seco*-grayanane (**1** and **2**), *ent*-labdane (**3** and **4**), mollane (**5**), leucothane (**6**, **12**, and **13**), 4,5-*seco*-*ent*-kaurane (**8**, **9**, and **14**), 1,10:2,3-di*seco*-grayanane (**10**), and *ent*-rosane (**15**) type diterpenoids showed distinct analgesic activities with the writhe percentage inhibitions above 50% (5.0 mg/kg, i.p.). Even at a lower dose of 0.04 mg/kg, pierisjaponins B (**2**), D (**4**), and 7-deoxyrosenonolactone (**15**) still exhibited stronger analgesic effects than morphine. This is the first time to report the analgesic activities of 1,5-*seco*-grayanane, mollane, *ent*-labdane, and *ent*-rosane diterpenoids. A preliminary structure-activity relationship is discussed. This work enlarges the structural diversity of diterpenoids in the Ericaceae family and provides new clues to develop novel potent analgesics.

Declaration of Competing Interest

The authors declare no competing financial interest.

This work was supported by NSFC (U1703109). Many thanks to the Analytical and Testing Center at HUST for UV, IR, CD, and crystal data measurements.

Appendix A. Supplementary Material

Supplementary data associated with this article can be found in the online version.

References

[1] J. Zhou, T. Liu, H. Zhang, G. Zheng, Y. Qiu, M. Deng, C. Zhang, G. Yao, Anti-inflammatory grayanane diterpenoids from the leaves of *Rhododendron molle*. J. Nat. Prod. 81 (2018) 151−161.

[2] Y. Li, Y. Liu, H. Yan, Y. Liu, Y. Li, H. Lv, S. Ma, J. Qu, S. Yu, Rhodomollins A and B, two diterpenoids with an unprecedented backbone from the fruits of *Rhododendron molle*. Sci. Rep. 6 (2016) 36752−36757.

[3] Y. Li, Y. Liu, J. Zhang, Y. Li, J. Jiang, S. Yu, S. Ma, J. Qu, H. Lv, Mollolide A, a diterpenoid with a new 1,10:2,3-di*seco*grayanane skeleton from the roots of *Rhododendron molle*. Org. Lett. 15 (2013) 3074−3077.

[4] W. Wang, Z. Wu, R. Chen, H. Li, H. Li, Y. Li, R. Li, H. Luo, Pierisformotoxins A–D, polyesterified grayanane diterpenoids from *Pieris formosa* and their cAMP-decreasing activities. Chem. Biodiversity 10 (2013) 1061−1071.

[5] C. S. Niu, Y. Li, Y. B. Liu, S. G. Ma, F. Liu, C. Li, H. B. Yu, X. J. Wang, J. Qu, S. S. Yu, Grayanane diterpenoids with diverse bioactivities from the roots of *Pieris formosa*. Tetrahedron 74 (2018) 375−382.

[6] C. H. Li, S. H. Luo, S. H. Li, J. M. Gao, New antifeedant grayanane diterpenoids from the flowers of *Pieris formosa*. Molecules 22 (2017) 1431−1439.

[7] C. Liu, C. Lei, Y. Zhong, L. Gao, J. Li, M. Yu, J. Li, A. Hou, Novel grayanane diterpenoids from *Rhododendron principis*. Tetrahedron 70 (2014) 4317−4322.

[8] J. Zhou, N. Sun, H. Zhang, G. Zheng, J. Liu, G. Yao, Rhodomollacetals A–C, PTP1B inhibitory

dite Lett. 19 (2017) 5352−5355.

[9] J. Zhou, G. Zhan, H. Zhang, Q. Zhang, Y. Li, Y. Xue, G. Yao, Rhodomollanol A, a highly oxygenated diterpenoid with a 5/7/5/5 tetracyclic carbon skeleton from the leaves of *Rhododendron molle*. Org. Lett. 19 (2017) 3935−3938.

[10] J. Zhou, J. Liu, T. Dang, H. Zhou, H. Zhang, G. Yao, Mollebenzylanols A and B, highly modified and functionalized diterpenoids with a 9-benzyl-8,10-dioxatricyclo[5.2.1.$0^{1,5}$]decane core from *Rhododendron molle*. Org. Lett. 20 (2018) 2063−2066.

[11] N. Sun, Y. Zhu, H. Zhou, J. Zhou, H. Zhang, M. Zhang, H. Zeng, G. Yao, Grayanane diterpenoid glucosides from the leaves of *Rhododendron micranthum* and their bioactivities evaluation. J. Nat. Prod. 81 (2018) 2673−2681.

[12] N. Sun, Y. Qiu, Y. Zhu, J. Liu, H. Zhang, Q. Zhang, M. Zhang, G. Zheng, C. Zhang, G. Yao, Rhodomicranosides A−I, analgesic diterpene glucosides with diverse carbon skeletons from *Rhododendron micranthum*. Phytochemistry 158 (2019) 1−12.

[13] N. Sun, G. Zheng, M. He, Y. Feng, J. Liu, M. Wang, H. Zhang, J. Zhou, G. Yao, Grayanane diterpenoids from the leaves of *Rhododendron auriculatum* and their analgesic activities. J. Nat. Prod. 82 (2019) 1849−1860.

[14] N. Sun, Y. Feng, Q. Zhang, J. Liu, H. Zhou, H. Zhang, G. Zheng, J. Zhou, G. Yao, Analgesic diterpenoids with diverse carbon skeletons from the leaves of *Rhododendron auriculatum*. Phytochemistry 168 (2019) 112113.

[15] Y. Li, Y. Liu, S. Yu, Grayanoids from the Ericaceae family: structures, biological activities and mechanism of action. Phytochem. Rev. 12 (2013) 305−325.

[16] X. Wang, R. Jiang, Z. Liu, W. Liu, M. Xie, S. Wei, G. She, Phytochemicals and biological activities of poisonous genera of Ericaceae in China. Nat. Prod. Comm. 9 (2014) 427−442.

[17] rom flowers of *Pieris japonica* and structure-activity relationships of antifeedant activity against *Pieris brassicae*. J. Agric. Food Chem. 65 (2017) 4456−4463.

[18] H. Hikino, K. Ito, T. Takemoto, Stereostructure of asebotoxin I and II, toxins of *Pieris japonica*. Chem. Pharm. Bull. 17 (1969) 854−855.

[19] T. Terai, K. Kiyono, K. Goto, Transformation of grayanotoxin III to the 1,5-*seco*-grayanotoxin derivative, grayanol B. Agric. Biol. Chem. 55 (1991) 2711−2715.

[20] H. Zhang, H. Wang, L. Wang, G. Bao, G. Qin, A new 1,5-*seco* grayanotoxin from *Rhododendron decorum*. J. Asian Nat. Prod. Res. 7 (2005) 87−90.

[21] Y. Zhu, H. Yan, X. Wang, Z. Zhang, H. Zhang, L. Chai, L. Li, J. Qu, Y. Li, Micranthanosides I and II, two novel 1,10-*seco*grayanane diterpenoids and their antinociceptive analogues from the leaves and twigs of *Rhododendron micranthum*. RSC Adv. 9 (2019) 18439−18450.

[22] C. Li, X. Niu, Q. Luo, M. Xie, S. Luo, Y. Zhou, S. Li, Novel polyesterified 3,4-*seco*-grayanane diterpenoids as antifeedants from *Pieris formosa*. Org. Lett. 12 (2010) 2426−2429.

[23] J. Zhou, Z. Zuo, J. Liu, H. Zhang, G. Zheng, G. Yao, Discovery of highly functionalized 5,6-*seco*-grayanane ditepenoids as potent competitive PTP1B inhibitors. Org. Chem. Front. 7 (2020) 829−837.

[24] Z. Wu, H. Li, W. Wang, X. Li, R. Li, Secopieristoxins A and B, two unusual diterpenoids with a new 9,10-*seco*grayanane skeleton from the fruits of *Pieris formosa*. Phytochem. Lett. 5 (2012) 87−90.

[25] Z. Wu, H. Li, W. Wang, H. Li, R. Chen, R. Li, H. Luo, Lyonin A, a new 9,10-*seco*grayanotoxin from *Lyonia ovalifolia*. Chem. Biodivers. 8 (2011) 1182−1187.

[26] A. Furusaki, N. Hamanaka, H. Miyakoshi, T. Okuno, T. Matsumoto, Leucothol A, an anthraditerpenoid from *Leucothoe grayana* Max. Chem. Lett. 1 (1972) 783−786.

[27] J. W. Burke, R. W. Doskotch, C. Z. Ni, J. Clardy, Kalmanol, a pharmacologically active diterpenoid

[28] S. Zhou, S. Yao, C. Tang, C. Ke, L. Li, G. Lin, Y. Ye, Diterpenoids from the flowers of *Rhododendron molle*. J. Nat. Prod. 77 (2014) 1185−1192.

[29] M. Zhang, Y. Zhu, G. Zhan, P. Shu, R. Sa, L. Lei, M. Xiang, Y. Xue, Z. Luo, Q. Wan, G. Yao, Y. Zhang, Micranthanone A, a new diterpene with an unprecedented carbon skeleton from *Rhododendron micranthum*. Org. Lett. 15 (2013) 3094−3097.

[30] Y. Li, Y. Liu, Y. Liu, C. Wang, L. Wu, L. Li, S. Ma, J. Qu, S. Yu, Mollanol A, a diterpenoid with a new C-*nor*-D-*homo*grayanane skeleton from the fruits of *Rhododendron molle*. Org. Lett. 16 (2014) 4320−4323.

[31] G. Yao, H. Zhai, L. Wang, G. Qin, Research progress in chemical constituents and biological activities of *Pieris* plants (Ericaceae). Sci. Online 1 1 (2006) 13−19.

[32] C. Niu, S. Liu, Y. Li, Y. Liu, S. Ma, F. Liu, L. Li, J. Qu, S. Yu, Diterpenoids with diverse carbon skeletons from the roots of *Pieris formosa* and their analgesic and antifeedant activities. Bioorg. Chem. 95 (2019) 103502.

[33] L. Wang, G. Qin, S. Chen, C. Li, Three diterpene glucosides and a diphenylamine derivative from *Pieris formosa*. Fitoterapia 72 (2001) 779−787.

[34] C. Niu, Y. Li, Y. Liu, S. Ma, F. Liu, L. Li, S. Xu, X. Wang, R. Wang, J. Qu, S. Yu, Pierisketolide A and pierisketones B and C, three diterpenes with an unusual carbon skeleton from the roots of *Pieris formosa*. Org. Lett. 19 (2017) 906−909.

[35] X. Lv, Y. Li, S. Ma, J. Qu, Y. Liu, L. Li, R. Wang, S. Yu, Isopimarane and *nor*-diterpene glucosides from the twigs and leaves of *Lyonia ovalifolia*. Tetrahedron 73 (2017) 776−784.

[36] Y. Gao, Y. Shen, X. Xu, J. Tian, H. Zeng, S. Lin, C. Liu, W. Zhang, Diterpenoids from *Gaultheria yunnanensis*. Phytochem. Lett. 8 (2014) 6−9.

[37] Z. Zhang, D. Guo, C. Li, J. Zheng, K. Koike, Z. Jia, T. Nikaido, Two diterpenoids from the roots of

[38] M. T., O. K. H., *In vitro* conversion of labdadienols into pimara- and rosa-dienes. Chem. Comm.(1968) 298−299.

[39] M. Liu, W. Wang, H. Sun, J. Pu, Diterpenoids from *Isodon* species: an update. Nat. Prod. Rep. 34 (2017) 1090−1140.

[40] T. Terai, K. Osakabe, M. Katai, K.-i. Sakaguchi, I. Narama, T. Matsuura, J. i. Katakawa, T. Tetsumi, Preparation of 9-hydroxy grayanotoxin derivatives and their acute toxicity in mice. Chem. Pharm. Bull. 51 (2003) 351−353.

[41] Y. Li, Y. Liu, J. Zhang, Y. Liu, S. Ma, J. Qu, H. Lv, S. Yu, Antinociceptive grayanoids from the roots of *Rhododendron molle*. J. Nat. Prod. 78 (2015) 2887−2895.

[42] C. Niu, Y. Li, Y. Liu, S. Ma, L. Li, J. Qu, S. Yu, Analgesic diterpenoids from the twigs of *Pieris formosa*. Tetrahedron 72 (2016) 44−49.

[43] Y. Li, Y. Zhu, Z. Zhang, Y. Liu, Y. Liu, J. Qu, S. Ma, X. Wang, S. Yu, Diterpenoids from the fruits of *Rhododendron molle*, potent analgesics for acute pain. Tetrahedron 74 (2018) 693−699.

[44] Y. Zhu, Z. Zhang, H. Yan, D. Lu, H. Zhang, L. Li, Y. Liu, Y. Li, Antinociceptive diterpenoids from the leaves and twigs of *Rhododendron decorum*. J. Nat. Prod. 81 (2018) 1183−1192.

[45] C. Niu, Y. Li, Y. Liu, S. Ma, X. Wang, F. Liu, S. Liu, J. Qu, S. Yu, Diverse epoxy grayanane diterpenoids with analgesic activity from the roots of *Pieris formosa*. Fitoterapia 133 (2019) 29−34.

[46] G. Zheng, J. Zhou, L. Huang, H. Zhang, N. Sun, H. Zhang, P. Jin, M. Yue, L. Meng, G. Yao, Antinociceptive grayanane diterpenoids from the leaves of *Pieris japonica*. J. Nat. Prod. 82 (2019) 3330−3339.

[47] G. Zheng, P. Jin, L. Huang, N. Sun, H. Zhang, H. Zhang, M. Yue, L. Meng, G. Yao, Grayanane diterpenoid glucosides as potent analgesics from *Pieris japonica*. Phytochemistry 171 (2020) 112234.

[48] S. Wang, S. Lin, C. Zhu, Y. Yang, S. Li, J. Zhang, X. Chen, J. Shi, Highly acylated diterpenoids with a

1560−1563.

[49] C. Niu, Y. Li, Y. Liu, S. Ma, F. Liu, L. Li, S. Xu, X. Wang, S. Liu, R. Wang, J. Qu, S. Yu, Biological and chemical guided isolation of 3,4-*seco*grayanane diterpenoids from the roots of *Pieris formosa*. RSC Adv. 7 (2017) 43921−43932.

[50] T. Dang, G. Zheng, Q. Zhang, P. Jin, H. Zhang, L. Su, D. Qin, G. Yao, Sesquiterpenoids with diverse carbon skeletons from the roots of *Cichorium glandulosum* and their anti-inflammatory activities. Fitoterapia 136 (2019) 104170−104177.

[51] Y. Teng, H. Zhang, J. Zhou, G. Zhan, G. Yao, Hebecarposides A−K, antiproliferative lanostane-type triterpene glycosides from the leaves of *Lyonia ovalifolia* var. *hebecarpa*. Phytochemistry 151 (2018) 32−41.

[52] S. Parsons, H. D. Flack, T. Wagner, Use of intensity quotients and differences in absolute structure refinement. Acta. Crystallogr. B. 69 (2013) 249−259.

[53] R. W. W. Hooft, L. H. Straver, A. L. Spek, Determination of absolute structure using Bayesian statistics on Bijvoet differences. J. Appl. Crystallogr. 41 (2008) 96−103.

[54] S. Fushiya, H. Hikino, T. Takemoto, Stereostructure of grayanol A and B, diterpenoids of *leucothoe grayana*. Tetrahedron Lett. 15 (1974) 183−186.

[55] W. G. Wang, H. M. Li, H. Z. Li, Z. Y. Wu, R. T. Li, New grayanol diterpenoid and new phenolic glucoside from the flowers of *Pieris formosa*. J. Asian Nat. Prod. Res. 12 (2010) 70−75.

[56] M. Katai, T. Terai, H. Meguri, A new diterpenoid from *Leucothoe grayana* Max. Chem. Lett. 14 (1985) 443−446.

[57] Y. Lai, Y. Xue, M. Zhang, J. Zhang, W. Tang, J. Liu, L. Lei, J. Yan, Z. Luo, J. Zuo, Y. Li, G. Yao, Y. Zhang, Scapiformolactones A–I: Germacrane sesquiterpenoids with an unusual Δ^3-15,6-lactone moiety from *Salvia scapiformis*. Phytochemistry 96 (2013) 378−388.

[58] *pus diplopappus*. Phytochemstry 38 (1995) 555−556.

[59] L. Wang, S. Chen, K. Cheng, C. Li, G. Qin, Diterpene glucosides from *Pieris formosa*. Phytochemistry 54 (2000) 847−852.

[60] J. Sakakibara, N. Shirai, T. Kiya, Diterpene glycosides from *Pieris japonica*. Phytochemistry 20 (1981) 1744−1745.

[61] Y. K. Kim, K. H. Son, J. Y. Nam, S. U. Kim, T. S. Jeong, W. S. Lee, S. H. Bok, B. M. Kwon, Y. J. Park, J. M. Shin, Inhibition of cholesteryl ester transfer protein by rosenonolactone derivatives. J. Antibiot. 49 (1996) 815−816.

[62] S. Chen, H. Zhang, L. Wang, G. Bao, G. Qin, Diterpenoids from the flowers of *Rhododendron molle*. J. Nat. Prod. 67 (2004) 1903−1906.

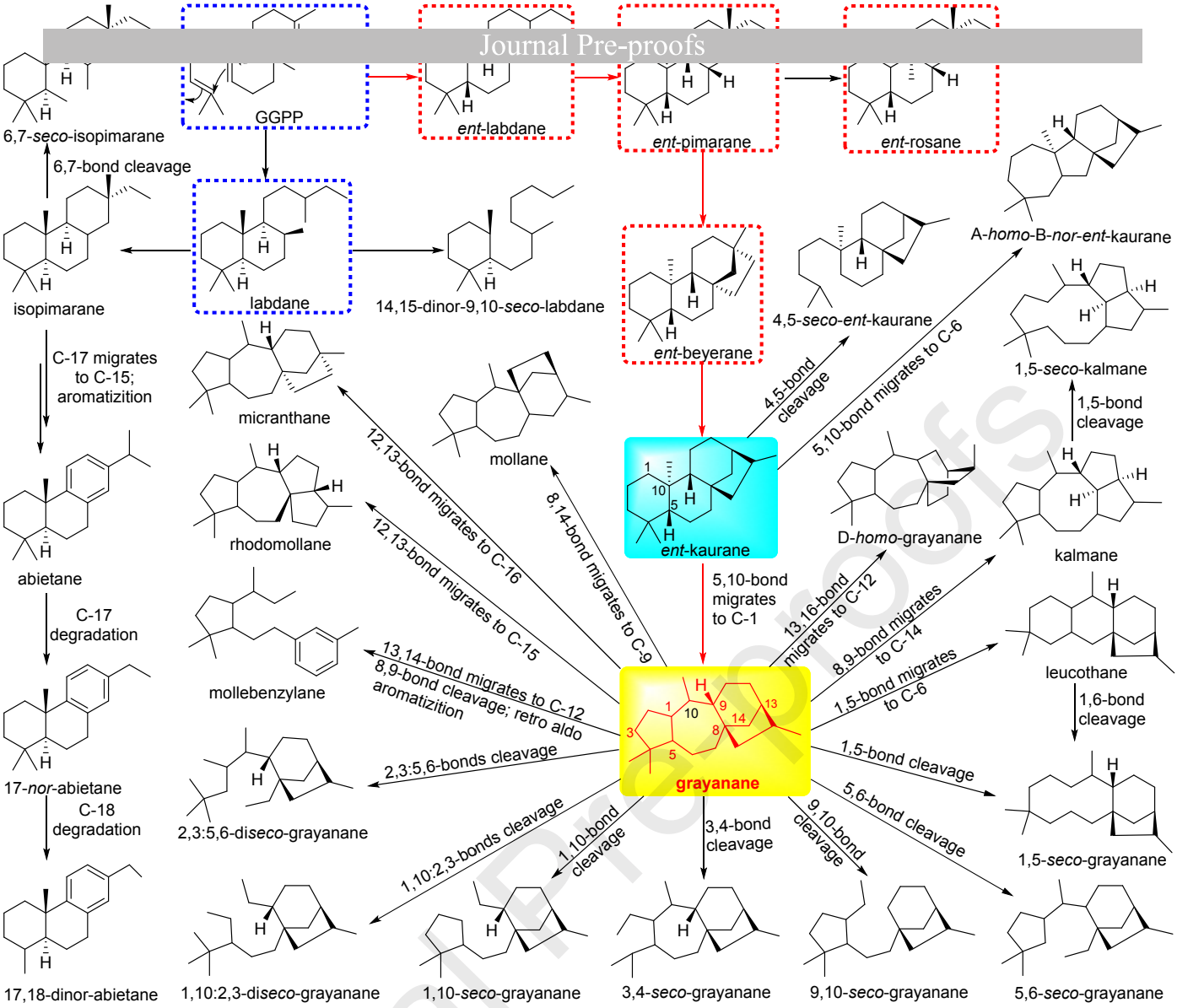

Fig. 1. Reported 25 Ericaceae diterpene carbon skeletons (except for five dashed ones) and their biogenetic relationships.

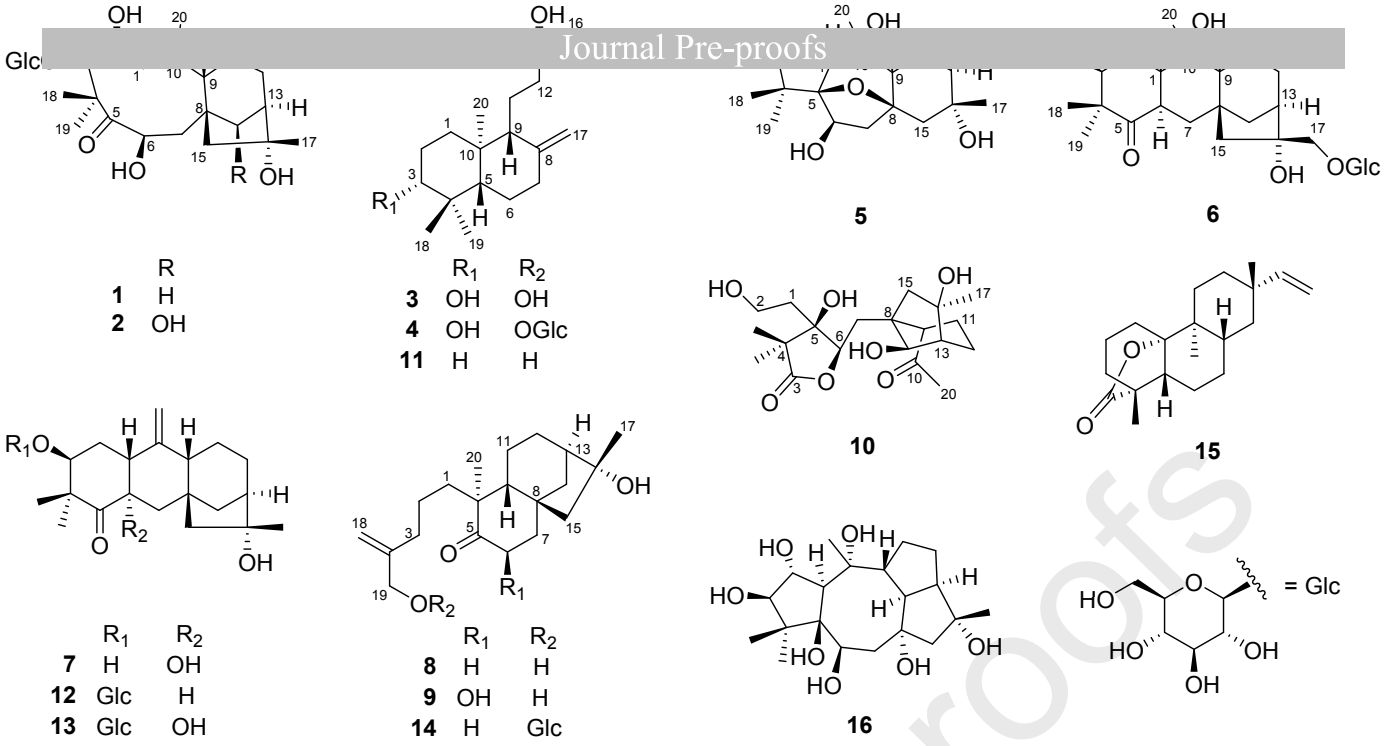

Fig. 2. Structures of diterpenoids **1**−**16**.

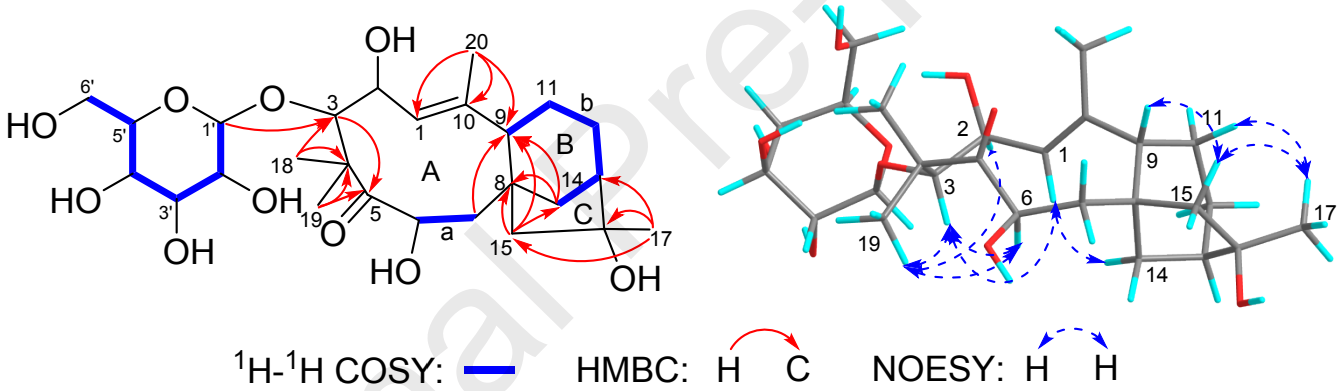

Fig. 3. Selected 2D correlations of pierisjapanin A (**1**).

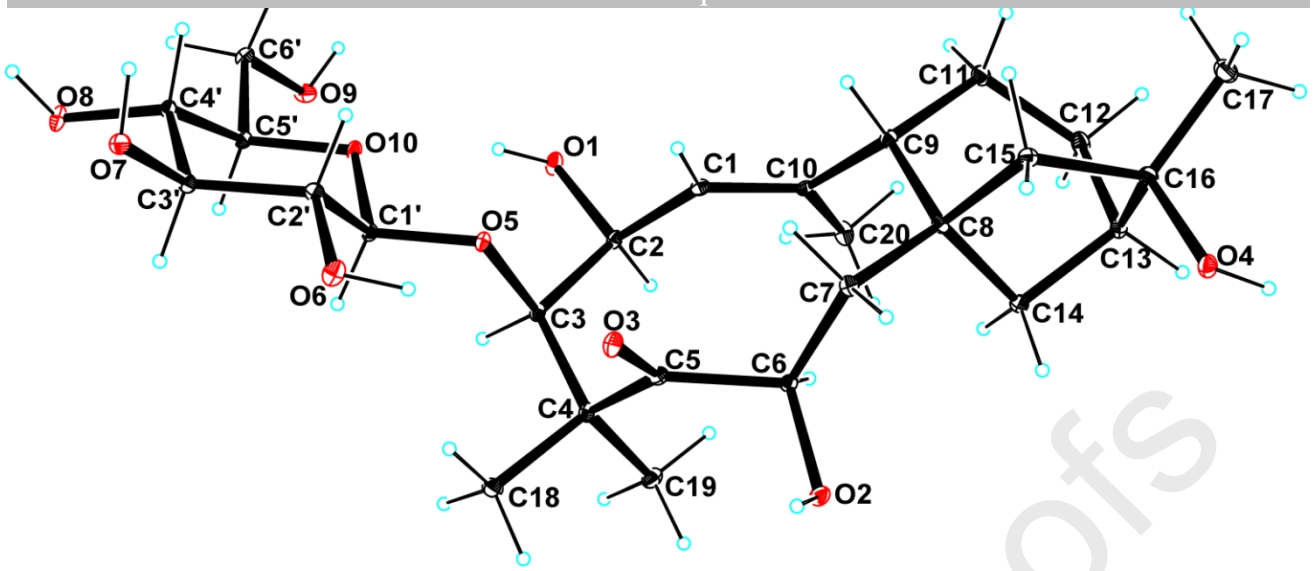

Fig. 4. Crystal structure of pierisjaponin A (**1**) (ellipsoids shown at the 10% probability level).

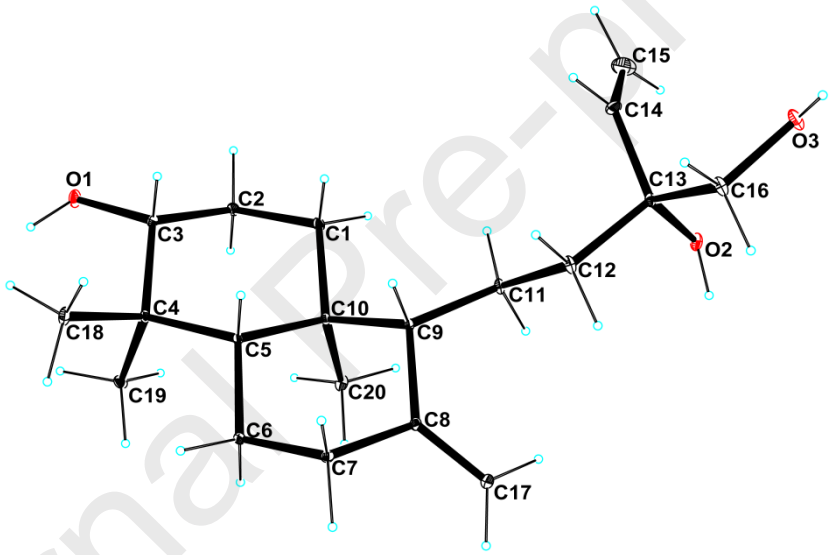

Fig. 5. Crystal structure of pierisjaponin C (**3**) (ellipsoids shown at the 10% probability level).

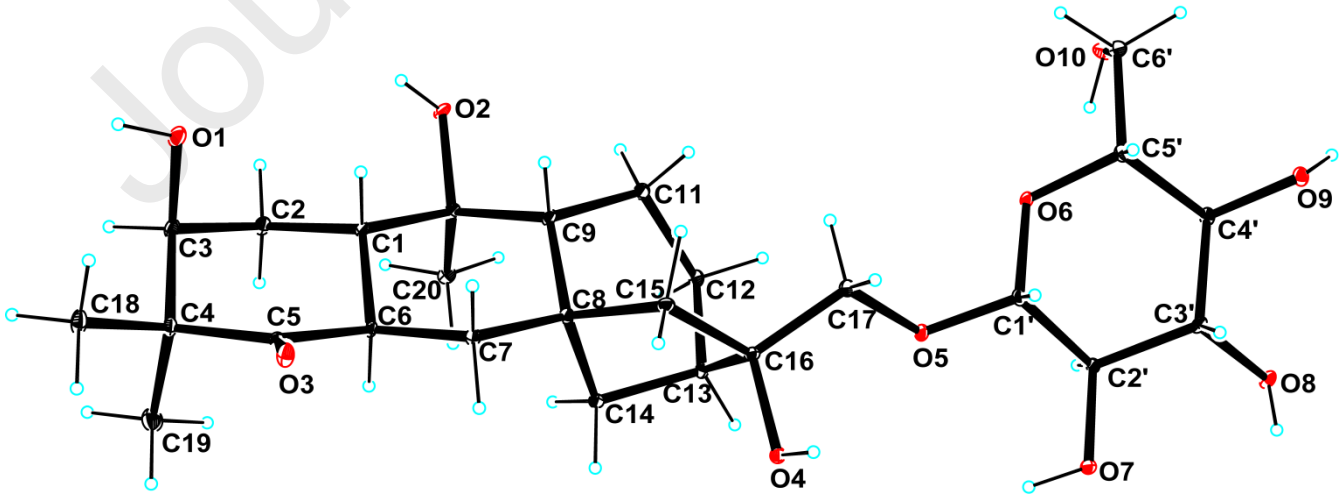

Fig. 6. Crystal structure of pierisjaponin F (**6**) (ellipsoids shown at the 10% probability level).

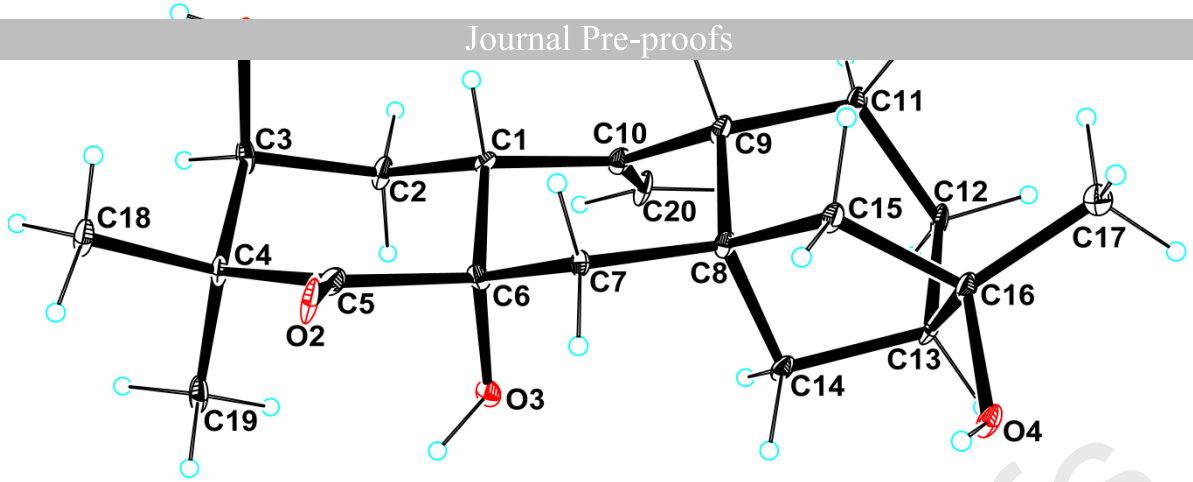

Fig. 7. Crystal structure of pierisjapanin G (**7**) (ellipsoids shown at the 10% probability level).

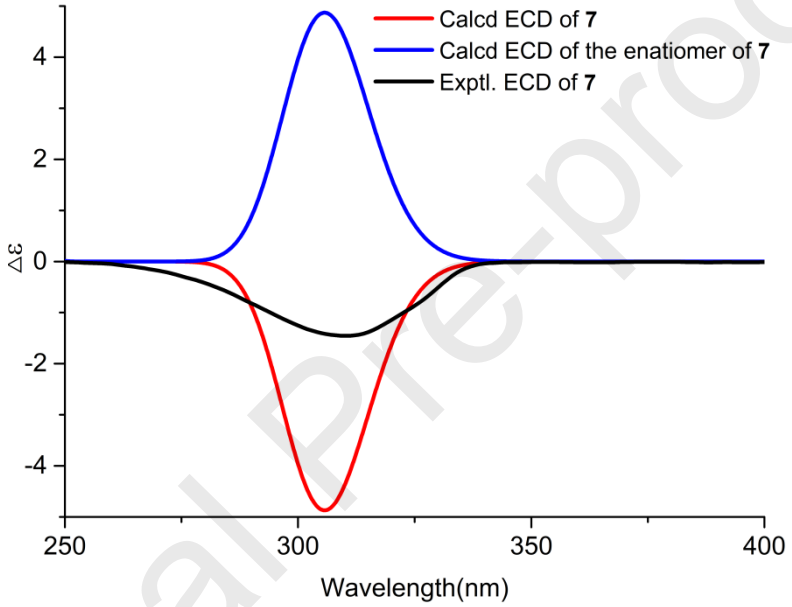

Fig. 8. The experimental and calculated ECD curves of pierisjapanin G (**7**) and its enantiomer.

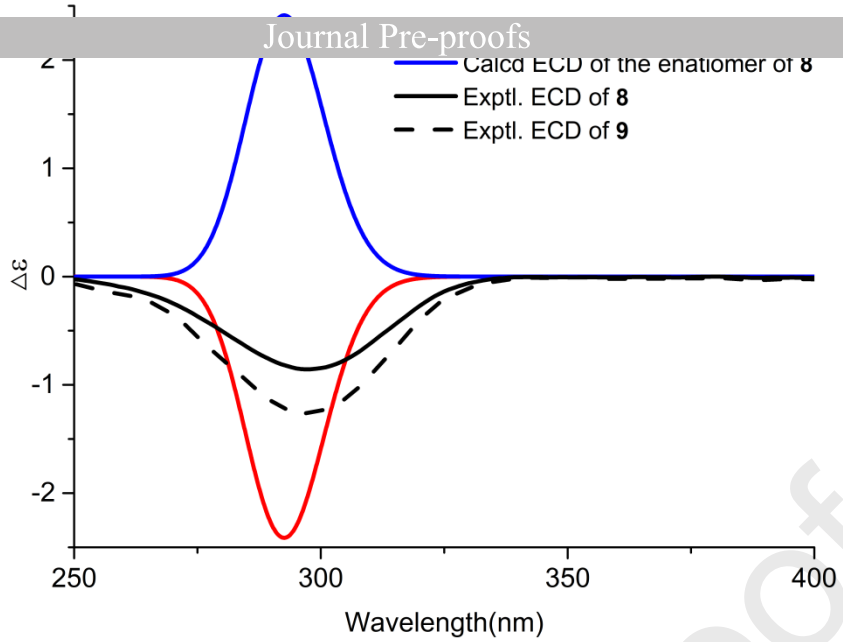

Fig. 9. The experimental ECD curves of pierisjaponins H (**8**) and I (**9**) and the calculated ECD curves of pierisjaponin H (**8**) and its enantiomer.

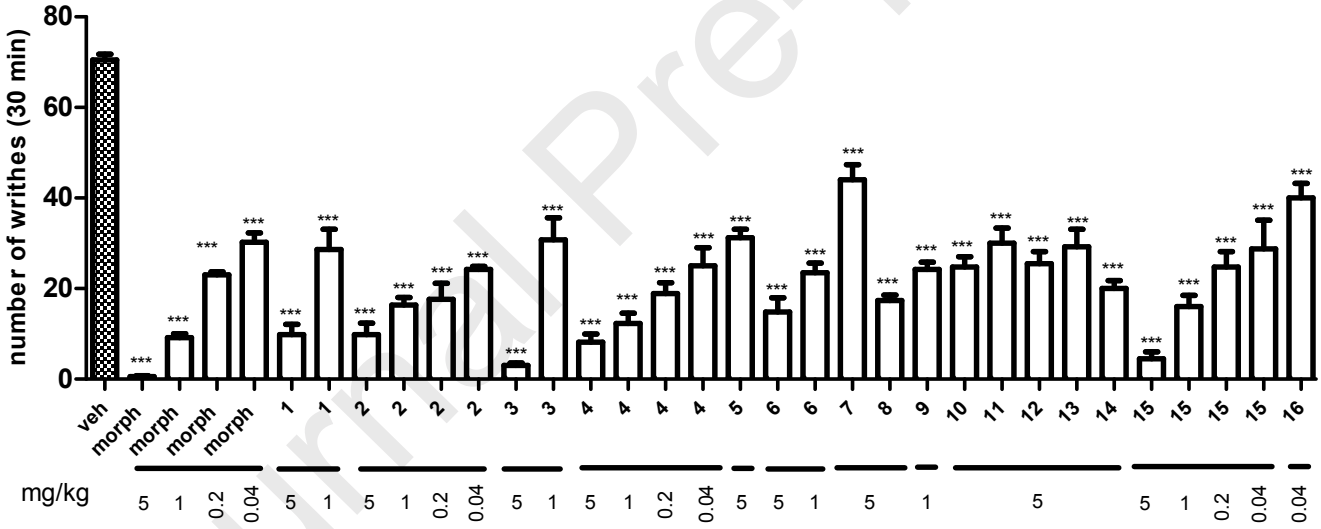

Fig. 10. Analgesic activities of diterpenoids **1**−**16** from *P. japonica* in the writhing model. n = 10, morphine (morph, positive control), ***$p < 0.001$, vs vehicle (veh).

Table 1

^{1}H NMR data (δ in ppm, multi. J in Hz) of pierisjaponins A–F (**1**–**6**) in CD_3OD (400 MHz).

Position	1	2	3	4	5	6
1α	5.02, br s	5.13, br s	1.80, dd (11.0, 3.1)	1.56, m	1.92, overlap	
1β			1.18, dd (11.0, 6.6)	1.48, m		1.85, overlap
2α	4.67[a], br s	4.67[a], br s	1.60, overlap	1.60, overlap	2.26, dt (13.4, 7.8)	2.04, m
2β			1.65, overlap	1.93, ddd (14.3, 5.8, 1.1)	1.84, dt (13.4, 5.3)	2.04, m
3α	3.83, br s	3.86, br s			3.59, dd (7.8, 5.3)	3.88, d (3.6)
3β			3.18, dd (9.1, 7.0)	3.35, overlap		
5			1.10, dd (12.5, 2.6)	1.60, dd (12.4, 2.3)		
6α	4.23, br s	4.40, br s	1.39, td (12.5, 4.9)	1.37, overlap	4.16, dd, (7.3, 2.3)	2.50, td (12.1, 2.8)
6β			1.73, overlap	1.63, overlap		
7α	1.51, dd (11.4, 2.3)	2.01, dd (11.3, 2.4)	2.39, ddd (12.8, 3.9, 2.3)	2.38, ddd (12.7, 4.0, 2.3)	1.57, dd (15.2, 2.3)	1.72, dd (12.1, 2.8)
7β	2.54, br d (11.4)	2.03, dd (11.3, 4.0)	1.97, dt (12.8, 4.9)	1.99, ddd (12.7, 4.0, 4.5)	3.01, dd (15.2, 7.3)	1.43, t (12.1)
9β	2.01, overlap	2.21, d (6.7)	1.53, overlap	1.63, overlap		1.34, d (8.2)
11α	1.48, dt (13.4, 6.4)	1.45, dt (13.3, 5.8)	1.42, m	1.41, m	2.13, td (12.3, 2.9)	1.89, overlap
11β	1.87, dt (13.4, 6.4)	1.84, m	1.53, overlap	1.59, overlap	1.78, td (12.3, 7.1)	1.63, overlap
12α	1.68, m	1.82, m	1.26, m	1.26, m	1.68, ddd (12.3, 7.1, 5.9)	1.75, overlap
12β	1.76, overlap	1.85, m	1.77, overlap	1.79, m	1.49, td (12.3, 2.9)	1.44, d (12.1)
13α	1.96, d (2.6)	2.10, br s			1.90, overlap	2.11, d (3.2)
14α	2.03, d (11.4)	4.26, s	5.88, dd (17.5, 10.9)	5.90, dd (17.4, 10.9)	1.40, dd (11.7, 4.5)	1.62, d (14.0)
14β	1.73, d (11.4)				1.93, d (11.7)	1.68, dd (14.0, 3.2)
15α	1.62, d (13.9)	1.95, d (14.8)	5.16, dd (10.9, 1.7)	5.15, dd (10.9, 1.6)	1.55, d (13.6)	1.54, d (14.3)
15β	1.76, d (13.9)	1.88, d (14.8)	5.29, dd (17.5, 1.7)	5.30, dd (17.4, 1.6)	1.94, d (13.6)	1.65, d (14.3)
16a			3.38, d (11.1)	3.88, d (10.0)		
16b			3.42, d (11.1)	3.44, d (10.0)		
17	1.36, s	1.34, s	4.83, s;	4.81, s;	1.19, s	4.23, d (10.2);
			4.62, s	4.60, s		3.53, d (10.2)
18	1.34, s	1.34, s	0.97, s	0.93, s	1.21, s	1.07, s
19	1.40, s	1.41, s	0.76, s	0.83, s	1.14, s	1.20, s
20	2.05, s	1.99, s	0.70, s	0.71, s	1.34, s	1.28, s
1′	4.48, d (7.6)	4.47, d (7.5)		4.26, d (7.7)	4.24, d (7.7)	4.29, d (7.7)
2′	3.33, overlap	3.32, overlap		3.21, dd (9.0, 7.7)	3.22, dd (9.2, 7.7)	3.23, dd (8.8, 7.7)
3′	3.44, t (8.4)	3.43, t (8.2)		3.34, overlap	3.34, overlap	3.28, overlap
4′	3.35, overlap	3.34, overlap		3.28, overlap	3.29, t (8.7)	3.28, overlap
5′	3.33, overlap	3.34, overlap		3.27, overlap	3.23, overlap	3.36, overlap
6′a	3.85, dd (11.3, 1.8)	3.84, dd (11.6, 1.4)		3.87, dd (11.6, 1.1)	3.85, dd (11.9, 2.1)	3.87, dd (12.0, 2.7)
6′b	3.68, dd (11.3, 5.3)	3.68, dd (11.6, 4.2)		3.66, dd (11.6, 5.3)	3.67, dd (11.9, 5.7)	3.66, dd (12.0, 4.7)

[a] Assigned by the NOESY data.

Table 2

^{13}C NMR data of pierisjaponins A−J (**1**–**10**) in CD_3OD (100 MHz).

Position	**1**	**2**	**3**	**4**	**5**	**6**	**7**	**8**	**9**	**10**
1	128.1[a]	128.9[a]	38.5	33.0	52.4	50.1	45.8	39.1	38.1	35.8
2	[c]	[c]	28.8	27.1	36.6	28.7	28.6	24.3	24.2	58.5
3	93.9[b]	94.4[b]	79.7	77.0	89.1	78.8	77.6	34.6	34.7	183.8
4	51.5[a]	52.4[a]	40.3	38.9	49.3	50.9	50.1	150.3	150.3	48.9
5	214.5	214.8[a]	56.3	49.9	93.7	218.2	215.7	218.8	216.1	80.0
6	70.7	70.5	25.4	25.3	77.9	45.9	80.0	38.2	71.9	85.4
7	48.4[b]	43.3[b]	39.5	39.0	48.1	40.3	38.9	38.3	48.1	33.0
8	50.2	56.1	149.5	149.8	84.4	44.7	46.8	45.5	45.2	51.8
9	56.8	58.7	58.8	58.7	53.9	55.2	51.6	48.0	48.0	56.3
10	146.0[a]	144.8[a]	40.8	40.8	72.4	76.5	150.8	53.8	53.5	214.3
11	23.9	22.8	18.5	18.3	27.5	19.5	22.5	20.5	20.0	21.7
12	27.0	27.6	37.2	37.9	28.9	26.7	26.0	27.4	27.5	25.9
13	49.5	54.5	77.3	76.6	47.4	47.0	50.7	49.5	49.7	54.2
14	36.5	80.8	143.1	142.9	33.0	37.0	45.4	37.5	38.4	81.5
15	58.4	57.3	114.6	114.5	48.0	53.2	56.5	56.9	57.2	52.4
16	80.4	81.6	69.8	77.4	74.4	82.1	79.6	80.1	79.5	82.0
17	24.3	23.4	107.8	107.6	28.8	75.1	24.1	24.6	24.5	23.7
18	27.3[a]	26.8[a]	29.0	29.4	19.6	21.9	23.5	109.9	109.9	18.5
19	21.5[a]	22.1[a]	16.3	23.0	26.9	25.8	27.6	65.9	65.9	22.4
20	17.3	17.3	15.2	15.1	31.6	20.3	107.9	24.9	25.1	30.9
1′	106.0[b]	106.3[b]		105.1	105.9	105.5				
2′	75.8	75.8		75.3	75.6	75.4				
3′	77.6	77.6		78.1	78.0	78.2				
4′	71.4	71.4		71.8	71.9	71.8				
5′	78.3	78.3		78.0	77.9	78.0				
6′	62.4	62.4		62.9	63.0	62.9				

[a] Assigned by the HMBC data. [b] Assigned by the HSQC data. [c] Not shown in the ^{13}C NMR spectra.

Tal

^{1}H NMR data (δ in ppm, multi. J in Hz) for pierisjaponins G–J (**7**–**10**) in CD_3OD (400 MHz).

Position	**7**	**8**	**9**	**10**
1	2.61, t (12.7)	1.64, m; 1.30, m	1.72, m; 1.34, m	1.84, t (7.1)
2α	1.71, overlap	1.60, m; 1.55, m	1.65, m; 1.30, m	3.80, d (7.1)
2β	2.48, td (12.7, 2.3)			3.82, d (7.2)
3	3.84, dd (3.3, 2.3)	2.02, m	2.04, m	
6α		2.70, ddd (15.4, 13.5, 6.9)	4.50, dd (13.4, 6.0)	4.25, d (9.6)
6β		2.24, ddd (15.4, 4.3, 3.0)		
7α	1.69, d (12.0)	1.78, overlap	1.70, dd (6.3, 6.0)	1.93, dd (15.8, 9.6);
7β	1.85, d (12.0)	1.82, overlap	2.02, dd (13.4, 6.3)	2.30, d (15.8)
9β	2.01, d (6.3)	1.75, m	1.65, m	3.11, d (8.8)
11α	1.79, overlap	1.68, m	1.71, m	1.84, m
11β	1.61, overlap	1.57, m	1.56, m	1.63, m
12α	1.79, overlap	1.66, m	1.72, m	1.57, m
12β	1.54, overlap	1.61, m	1.62, m	1.71, m
13α	1.78, overlap	1.96, overlap	2.00, overlap	1.96, m
14α	1.78, overlap	1.98, d (11.4)	2.09, d (10.9)	4.73, s
14β	1.71, overlap	1.88, d (11.4)	2.01, d (10.9)	
15α	1.80, d (14.4)	1.67, d (14.3)	1.70, d (15.2)	1.92, d (15.8)
15β	1.67, d (14.4)	1.63, d (14.3)	1.66, d (15.2)	1.88, d (15.8)
17	1.36, s	1.39, s	1.39, s	1.38, s
18	1.06, s	4.99, s; 4.82, s	4.99, s; 4.83, s	1.18, s
19	1.35, s	3.98, s	4.00, s	1.21, s
20	4.98, s; 4.95, s	1.23, s	1.25, s	2.20, s

Highlights

- Sixteen diterpenoids belonging to eight diverse carbon skeletons were isolated.
- Pierisjaponins A and B represent the first 1,5-*seco*-grayanane diterpenoid glucosides.
- Pierisjaponin E is the first mollane diterpene glucoside.
- This is the first report of *ent*-labdane and *ent*-rosane type diterpenoids from the Ericaceae plants.
- All the isolates showed significant analgesic activities.

Graphical abstract

Structurally Diverse Diterpenoids from *Pieris japonica* as Potent Analgesics

Guijuan Zheng, Pengfei Jin, Lang Huang, Qihua, Zhang, Lingkui Meng, Guangmin Yao*

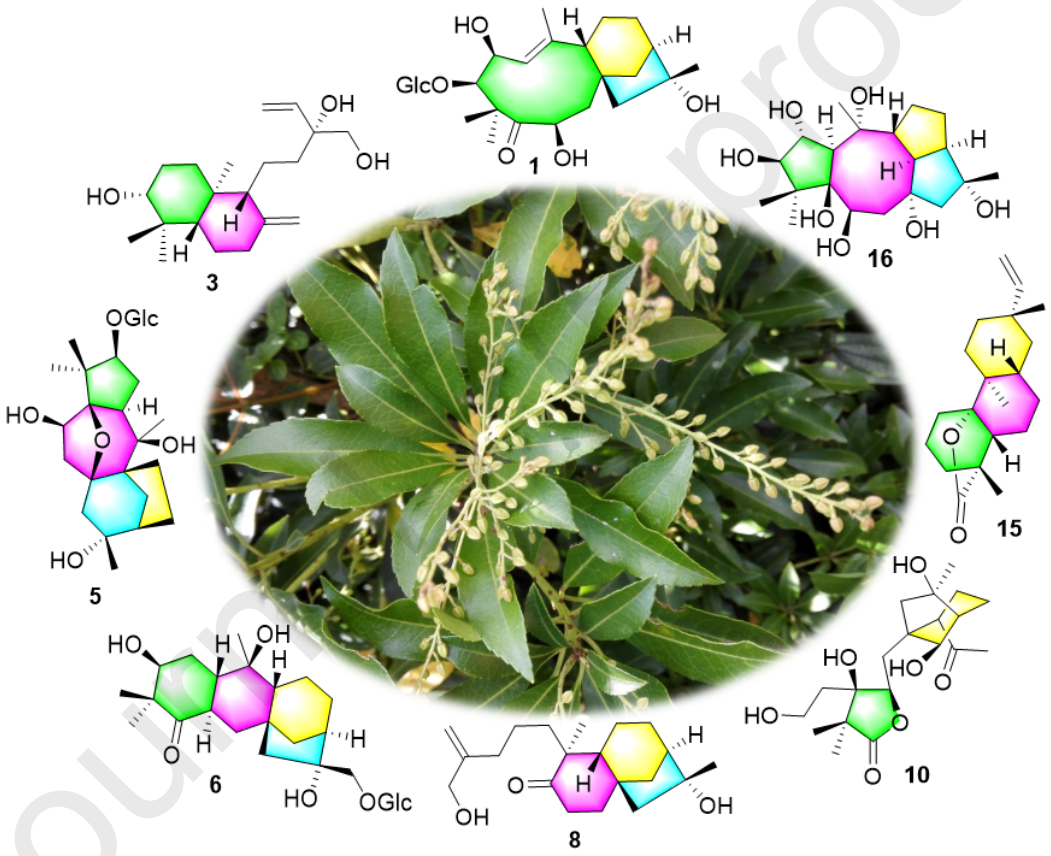

Sixteen diterpenoids belonging to eight diverse carbon skeletons, 1,5-*seco*-grayanane, *ent*-labdane, mollane, 4,5-*seco*-*ent*-kaurane, leucothane, 1,10:2,3-di*seco*-grayanane, *ent*-rosane, and kalmane, were characterized from *Pieris japonica*. Pierisjaponins A (**1**) and B (**2**) represent the first 1,5-*seco*-grayanane diterpenoid glycosides and showed unusual NMR phenomena. Pierisjaponin E (**5**) is the first mollane diterpenoid glycoside. This is the first report of *ent*-labdane (**3**, **4**, and **11**) and *ent*-rosane (**15**) type diterpenoids from the Ericaceae plants, which provided the precursor of the Ericaceae diterpenoids and enlarged the chemical diversity of Ericaceae diterpenoids. All the 16 isolates showed potent analgesic activities. A preliminary

structure-activity relationship is discussed, which provided new clues to design novel analgesics based on the Ericaceae diterpenoids.

Declaration of Competing Interest

The authors declare no competing financial interest.